T.R.

GEBZE TECHNICAL UNIVERSITY

INSTITUTE OF BIOTECHNOLOGY

DESIGN AND DEVELOPMENT OF A PERSONALIZED MEDICINE ORIENTED MICROFLUIDIC ORGAN ON A CHIP PLATFORM

AHMET AKİF KIZILKURTLU

A THESIS SUBMITTED FOR THE DEGREE OF

MASTER OF SCIENCE

DEPARTMENT OF BIOTECHNOLOGY

GEBZE

2020

T.R.

GEBZE TECHNICAL UNIVERSITY

INSTITUTE OF BIOTECHNOLOGY

DESIGN AND DEVELOPMENT OF A PERSONALIZED MEDICINE ORIENTED MICROFLUIDIC ORGAN ON A CHIP PLATFORM

AHMET AKİF KIZILKURTLU

A THESIS SUBMITTED FOR THE DEGREE OF MASTER OF SCIENCE

DEPARTMENT OF BIOTECHNOLOGY

THESIS SUPERVISOR

ASSOC. PROF. DR. ALİ AKPEK

GEBZE

2020

T.C.

GEBZE TEKNİK ÜNİVERSİTESİ

BİYETOKNOLOJİ ENSTİTÜSÜ

KİŞİSELLEŞTİRİLMİŞ TIBBA YÖNELİK MİKRO AKIŞKAN ÇİP ÜSTÜ ORGAN PLATFORMUNUN TASARIM VE GELİŞTİRİLMESİ

AHMET AKİF KIZILKURTLU

YÜKSEK LİSANS TEZİ

BİYOTEKNOLOJİ ANABİLİM DALI

DANIŞMANI

DOÇ. DR. ALİ AKPEK

GEBZE

2020

GEBZE TEKNİK ÜNİVERSİTESİ	YÜKSEK LİSANS JÜRİ ONAY FORMU

GTÜ Biyoteknoloji...Enstitüsü Yönetim Kurulu'nun ...../...../..... tarih ve ...../..... sayılı kararıyla oluşturulan jüri tarafından ..29../.01.../.2020. tarihinde tez savunma sınavı yapılan Ahmet Akif.....KIZILKURTLU.....'ın tez çalışması .....Biyoteknoloji.....Anabilim Dalında YÜKSEK LİSANS tezi olarak kabul edilmiştir.

JÜRİ

ÜYE
(TEZ DANIŞMANI) : Doç. Dr. Ali AKSEK

ÜYE : Dr. Öğr. Üyesi Ayça Bal Öztürk

ÜYE : Dr. Öğr. Üyesi Emine Alarçin

ONAY

Gebze Teknik Üniversitesi Biyoteknoloji Enstitüsü Yönetim Kurulu'nun

...../...../..... tarih ve ...../..... sayılı kararı.

SUMMARY

Bringing a drug in health sector costs about 2 billion dollars and the process lasts 12 to 15 years. One of the most important steps of these studies is preclinical testing which is also highly crucial in cosmetic toxicity tests and disease modelling tests. Organs on chip platforms that interconnect bioengineering, chemical engineering and material engineering are the most recent discovery, which have demonstrated their capability for drug development, cosmetic toxicity testing, and disease modelling implementation instead of animal models.

In this study, PMMA utilized chip was fabricated and GelMA - alginate mixture containing scaffold was fabricated via using a 3D bio-printer and then inserted in the chip system in order to mimic tissue scaffold. Afterwards, mouse fibroblast cells (3T3) were cultured on the chip system, the system was constantly fed with growth culture by using syringe pump. As a control experiment a Petri dish was used and instead of the designed organ on a chip platform. The results were compared with each other. The study was conducted as four different stages: First, an original design for the organs on a chip system was developed and realized. Second, several biomaterials were developed. These biomaterials are 7% - 5% GelMA - alginate mixture, 7% - 4% GelMA - alginate mixture, 5% - 4% GelMA - alginate mixture and 10% - 7% GelMA - alginate mixture. As a third step, these biomaterials were placed to Petri dishes and organs on a chip platforms and fibroblast cells were introduced to both systems. Finally, cell viability results were compared with each other. Results proved that the integrity of the scaffolds were more stable in the chip system and the cell viability was higher compared to Petri dishes. The research indicated an obvious supremacy of organs on chip platforms than 2D platforms thus providing a great promise for reducing the usage of animal in preclinical testing and disease modelling in the years to come. It is proven that in order to achieve more accurate results instead of 2D platforms, 3D structures such organs on a chip platform should be favored.

Keywords: microfluidics, organ-on-a-chip, 3D bio printing, disease modelling, animal testing

ÖZET

Bir ilacın sağlık sektörüne girişi 2 milyar dolar civarına mal olup, 12 ile 15 yıl arasında bir zaman alabilmektedir. Bu çalışmaların en önemli basamaklarından birisi klinik öncesi testleridir ki çalışmaların bu basamağı; kozmetik toksisite testlerinde ve hastalık modellemeleri testlerinde de müşterektir. Birçok mühendislik disiplinlerini birleştiren ve bu disiplinlerin ortak ürünü olan çip üzeri organ platformları; ilaç geliştirme, kozmetik toksisite testleri ve hastalık modellemesi çalışmalarında deney hayvanları yerine kullanılabilecek özelliklere sahip olduğunu kanıtlamıştır.

Bu çalışmada, PMMA malzemesi kullanılarak organ çipi üretimi yapıldı, 3B biyoyazıcı vasıtasıyla jelatin metakrilat ve sodyum aljinat karışımı içeren solüsyon hazırlanarak doku iskelesi basıldı ve çip sistemi içerisine entegre edildi. Ardından, fare fibroblast hücreleri (3T3) çip içerisinde kültüre edilerek şırınga pompası yardımıyla devamlı hücre medyumu ile beslendi ve petri kabıyla kıyas edildi. Çalışma dört farklı bölüm olarak yürütüldü. İlk olarak, çip üzeri organ orjinal bir tasarımla geliştirilip üretildi. İkinci olarak, 10%- 7% GelMA-Sodyum Aljinat, 7%- 5% GelMA-Sodyum Aljinat, 7%- 4% GelMA-Sodyum Aljinat ve 5%- 4% GelMA-Sodyum Aljinat karışımı olmak üzere dört adet biyomalzeme üretildi. Üçüncü olarak, üretilen biyomalzemeler çip üzeri organ platformu ve petri kabına yerleştirildi, ardından fare fibroblast hücreleri iki sisteme birden kültüre edildi. Son olarak, iki sistem hücre canlılığı oranı için karşılaştırıldı. Çip sistemi hem doku iskelesinin bütünlüğünü koruması açısından hem de hücre canlılığı oranı açısından petriden daha başarılı olmuştur. Mezkûr çalışma çip üzeri organ platformunun iki boyutlu platformlara göre net bir şekilde daha üstün olduğunu gösterdi. Bu durum, gelecek yıllarda preklinik testlerde ve hastalık modellemelerinde deney hayvanlarının kullanımını azaltacağına işaret etmektedir. Bu daha isabetli sonuçlar almak için iki boyutlu platformlar yerine çip üzeri organlar gibi üç boyutlu yapılar tercih edilmesi gerektiğini kanıtlamaktadır.

Anahtar Kelimeler: mikro akışkanlar, organ üzeri çip, 3B biyo-basım, hastalık modellemesi, hayvan deneyleri

ACKNOWLEDGEMENTS

I really would like to express my greatest and humble gratitude towards my dear supervisor, Associate Professor Ali AKPEK. He was my mentor during my postgraduate program, I have learned from him a lot, not only about science and engineering but also about entrepreneurship and no wonder about life. I would never be able to complete this research and experiment without his support, guidance, aid, and of course encouragement.

I want to state my deepest thanks to Assistant Professor Ayça BAL ÖZTÜRK for essential helps in the process of fabrication of the tissue scaffold. Dear ma'am welcomed us in her laboratory and she attended every step of the process warmheartedly. In addition, I want to thank Gözde YEŞİLTAŞ and Soner TÜRKÜNER for their vital aids and collaboration in the processes of cell culture and cell viability imagining.

This project was supported by TUBITAK project no: 217M756. Therefore, I would like to express my gratitude to TUBITAK to support our research.

Finally, I wish to express my warmest and sincerest gratitude to my dear family. They were always with me to support in the process of "*per ardua ad astra*" and they have always believed in me whatever and whenever I am on to something.

TABLE OF CONTENTS

LIST of ABBREVIATIONS

Abbreviations and Acronyms		Explanations
°C	:	Centigrade
µl	:	Micro-liter
µm	:	Micro-meter
2D	:	Two-dimensional
3D	:	Three-dimensional
ADME	:	Absorption, distribution, metabolism, and Excretion
cm	:	Centimeter
CO_2	:	Carbon Dioxide
DMI	:	Deuterium Metabolic Imaging
DNA	:	Deoxyribonucleic Acid
DPBS	:	Dulbecco's phosphate-buffered salin
EDTA	:	Ethylenediaminetetraacetic acid
g	:	Gram
GelMA	:	Gelatin Methacrylate
h	:	Hour
L	:	Liter
ml	:	Milliliter
mm	:	Millimeter
PBS	:	Phosphate Buffered Saline
PMMA	:	Polymethyl methacrylate
PDMS	:	Polydimethylsiloxane
PMT	:	Photomultiplier Tube
psi	:	Pounds per square inch
RGD	:	Arginylglycylaspartic acid
rpm	:	Revolutions per minute
USD	:	United States of American Dollar
UV	:	Ultraviolet

LIST OF FIGURES

LIST of TABLES

1. INTRODUCTION

Developing and designing suitable platform for remodeling a disease, creating a diagnosis tool and design tailor made drugs is most important part of the process. Therefore, the procedures follow similar pathways. In drug development, potentially effective drug candidate is identified; lead compounds are designed, modelled, developed, and optimized via utilizing *in silico* techniques. After that, preclinical testing is performed with compound libraries in order to detect which of the library member shows effectiveness against the specific target in question.

Preclinical testing consists of two different implementations, which are *in vitro* analyses by using proper cell line models and *in vivo* studies via using animal models. All of these processes are conducted to determine not only validity and toxicity, but also pharmacokinetic and pharmacological characteristics testing to analyze the absorption, distribution, metabolism and excretion rate of the substance, which is crucial for detecting the basic safety and potential usefulness of the drug (candidate).

Eventually, the compounds that are passed the previous procedures are subjected to clinical trials (human trials) in order to specify the ultimate validity, effectivity, and usefulness of the drug. Although the investigation and researches on new drug candidates for acute, chronic and genetic diseases are being performed accelerando, the rate of finding successful and effective drug reagents is dramatically low [24], [27], [37]. That is because either lack of clinical efficacy or intolerable toxicity of the drug candidates during investigation process [20], [26].

Since the mentioned processes are expensive and time consuming [14], it is very important to detect the compounds that are potentially ineffective or have an unacceptable toxicity and dismiss in early stages of drug development. Therefore, development of *in vitro* cell-based testing methods is crucial and necessary to provide possibility to predict precisely for efficacy and safety of drug candidates. Cell cultures for both drug development and disease modelling can be categorized as 2D cell culture, 3D cell culture (involves 3D bio-printing technology), and microfluidic systems.

1.1. 2D Cell Cultures

First attempt of cell culturing method was developed and performed by Harrison in 1907, while he was investigating the origin of nerve fibers [19]. He extracted pre-differentiated neural tissue from frog embryos and placed in a drop of lymph hanging

from a sterile cover slip, kept sealed and in a moist chamber. That process showed that cells of interest could be cultured outside of the body when the growth and differentiation of the tissue continues [18]. After that, different kinds of methods were developed and applied for specific researches.

Main concept of 2D cell culture depends on growing cells in a culture flask or in a flat Petri dish that is attached to a plastic surface as a monolayer. Even though 2D cell culture is inexpensive compared to others, well established since it has been used since 1900s, easy to compare the results with previous ones, easy to implement and conduct observation and measurement, it has critical disadvantages. For instance, it dramatically lacks represent the real cell environments since it is on a flat surface that hinders cell growth and function because normally cells are surrounded by other cells in three dimensions.

In addition, 2D cell cultures are weak in drug development researches since 2D makes it unpredictable and consuming media cause exudation of waste, which can cause toxic waste products, low life span, increasing of dead cells, nutrition depletion and damage of the environment. Thus, the researches and effort are directed to create cell cultures in 3D.

1.2. 3D Cell Cultures

Cells cultures as modelled as three-dimensional show much closer structure to complex *in vivo* conditions. Because, three-dimensional cell cultures provide an artificial environment for cells to grow and interact with their surroundings in all three dimensions [2]. Hence, 3D cultures more accurately mimic the *in vivo* cells compared to 2D cell cultures, which was proven by some studies such as cell number monitoring, viability, morphology, proliferation, differentiation, cell-cell communication [29].

Furthermore, 3D cultures provide much better information about response to stimuli, drug metabolism, migration and invasion of tumor cells into surrounding tissues, angiogenesis stimulation and immune system evasion, gene expression, synthesis of amino acids and proteins, general cell function and *in vivo* relevance. Besides, three-dimensional cell cultures are available to be cultured much longer at least up to 4 weeks, which is maximum one week with 2D monolayer culture due to cell confluency. 3D cell culture models can be distinguished as whole animals and organotypic explant cultures, cell spheroids, micro carrier cultures and tissues-

engineered models [28]. Table 1. 1 shows the differences between 2D and 3D cell cultures.

Table 1. 1: The differences between 2D and 3D cell cultures [10]

2D *vs.* 3D	**2D Cell Culture**	**3D Cell Culture**
Advantages	• Long-studied technique and fast evaluation • Low-cost • Easy to implement and analyze • Suitable for mass production with high output	• Emulation of ECM • Mimicking natural environment of the cells and their interactions • Suitable for drug researches and tissue penetration applications • No requirement for redesign that reduces the cost
Disadvantages	• No ECM emulation • Lack capabilities of mimicking cell-cell interactions and cell-environment interactions • Unrealistic drug effects in the process • Inability of utilization in drug screening and testing experiments • Requires redesign and repetitive implementations that increases the cost	• Requires expensive and advanced lab tools • Not well-established system that causes low throughput of experiments

Generally, whole animal and organotypic explants are utilized for tissue-specific information. The model is important in terms of creating *in vivo* research, observe and understand the overall effects of the experiment (like cancer researches) on a living subject. However, the animal testing is not always successful, since they do not clearly indicate the ADME in human body and some disease cannot be precisely modelled such as brain, kidney and skin cancer [17]. More importantly, using of animal models is entirely focus of ethical and political discussions, since the experiments mostly cause pain, ultimate death and continuous subjection to specific light, temperature, and implementations. Moreover, animal care, housing, feeding and breeding are highly expensive and time-consuming. These reasons made the researchers face to necessity of finding alternative model for disease modelling, drug development, and other

applications. Thus, cellular spheroids has been started to be utilized for *ex vivo* 3D cultures, which can be generated from a wide range of cell types [11].

They are self-assembled spherical clusters of cell colonies and they can be created from single culture or co-culture techniques such as hanging drop, rotating culture, or concave plate methods. The spheroids are beneficial approach especially in cancer research, because it permits to be observed the discovery of morphological changes in transformed cells swiftly. Using of polarized epithelial cell culture is another method for 3D cell culture, which is based on using of human keratinocytes by isolating from skin and cultured on supportive biologicals such as collagen or de-epidermalised human dermis in order to sustain the native basement of membrane proteins, ability of adhesion and growth of keratinocytes.

3D cell cultures have extended the range of cell culture approaches and lots of researches has been conducted by using those methods, yet the methods lacked precision, mechanical stability and control, desired functionality and physiological and biochemical similarity to original human organs and tissues most importantly. Therefore, an innovative method that was inspired from 3D printing was developed as 3D bio printing. Figure 1.2 shows basic principle of 3D cell culturing.

1.3. 3D Bio-printing

It is considered the most advanced implementation technique of 3D cell culture, which gathers biology, medicine, mechanical, electrical and electronics engineering, and computer engineering disciplines' theoretical knowledge and applications in order to fabricate 3D structures. Charles W. Hull firstly described the technique by naming it as 'stereolithography' in 1986 [23]. The method was clarified as constructing thin layers of a material by curing with ultraviolet light sequentially printed in layers to form a solid 3D structure. Afterwards, the process was applied to generate sacrificial resin molds for the construction of 3D scaffolds from biological materials.

The development of the system has provided an opportunity to direct printing of materials into 3D scaffolds, which can be utilized for transplantation by using or not using seeded cells [36]. Then, it was followed by printing a form of tissue engineering, which opened a new pathway to new advances 3D printing technology, cell biology and materials science. Thus, stents and splints were fabricated by using 3D bio printing technology and successfully implanted to patients [34]. The concept of 3D bio printing

is based on precisely positioning of biological materials, biochemical factors, and living cells layer-by-layer via helping of control of the placement of functional components to build 3D living structures.

3D bio printing approaches can be categorized as biomimicry, autonomous self-assembly and mini-tissue building blocks. The disadvantages of 3D bio printing are printing molten plastics and metals to the printing of sensitive, living biological materials and reproducing the grift micro-architecture of extracellular matrix (ECM) components and multiple cell types in acceptable resolution to emulate biological function. Creating ECM in 3D cell cultures is considered most challenging part that must be fulfilled, which some biological materials are utilized such as collagen, alginate and synthetic polymers (polyethylene glycol, polylactic acid, polyethylene glycol methacrylate), alginate in order to mimic ECM [39]. Figure 1. 1 shows a real example of bio-printing process.

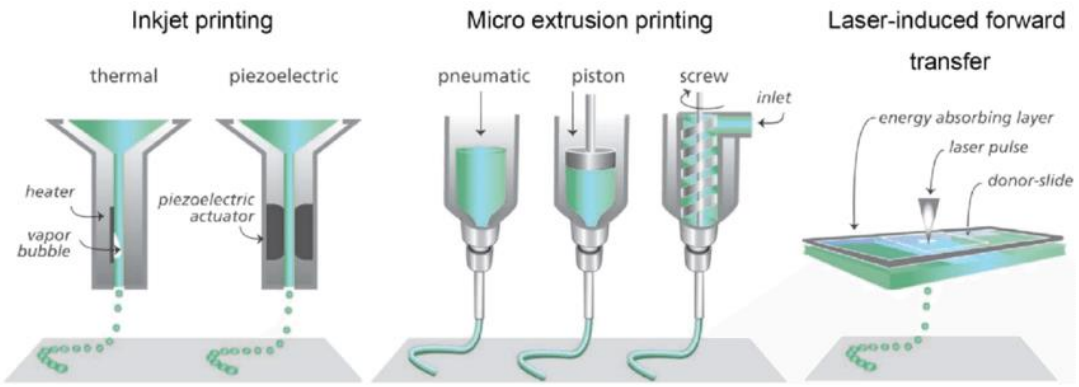

Figure 1.1: The most common 3D bio-printing fabrication techniques [7].

1.4. Micro-Fluidics Systems and Its Evolution Towards Organs on a Chip Platforms

Technology modernization has ushered in a new age in terms of acceleration in both science and industry. One of the most unique and necessary advancement was miniaturization. It has played a great role as one of the predominant research and implementation area in evolution of modern technology [16], [35]. This technology allows devices to have complex features and functionalities in a smaller size and volume with lower cost, less energy consumption and less occupying a place per

applied function. Furthermore, it requires much lower time to process, much smaller volume of required reactants and samples, multifunctionality by easily integrated with other tools and systems, lower fabrication and operational costs, high throughput, and maximum safety and reliability by having fewer external interconnects between the different parts. Microelectromechanical systems (MEMs) were the representatives of the miniaturization technology via having precise functionalities in both electrical and mechanical part of the system that cover wide range of implementation areas, such as physical, chemical, and biological domains [25].

MEMs technologies ensured the possibility of integration of small mechanical and electronic pieces to a single complex system, which performs electronic signal processing, sensing, and electromechanical actuation. That shows the importance of the technology by substituting traditional methods that perform the mentioned processes in separated and partial functional blocks. There is a specific system that are related and associated with life science. MEMs are used in systems implemented to biological assays and fluid manipulation (interstitial fluids, blood flows and cell manipulation, DNA analysis, toxins detection, diseases diagnosis and treatment, drug discovery, effectivity and delivery tests [32], [40] are named bio-MEMS [45] and microfluidics [43]. Microfluidics is the scientific field of the microsystems technology, which aim to research and control of fluids in hydraulically and geometrically small systems, with lengths generally is about a few micrometers up to a few millimeters or centimeters.

Besides, the volume of fluid in the microsystem is nanoliters and the flow rates differ from few nanoliters per second to nanoliters per hour range. Since this technology has strict specifications in terms of precision of fabrication and compatibility between the different materials used to manufacture them, probable interactions between mechanical and electronic parts and the fluids-biological systems of interest, it draws a great attention of researches of physical, chemical, and biological implementation areas [48]. Microfluidic systems are composed of four main components:

Microfluidic pumps that is necessary in order to drive the fluids along the system. Microfluidic valves that is important to control and direct the flow as desired. Microfluidic channels and chambers that are the passive and the primary fluidic interconnecting components of these systems, and active microfluidic components that integrated with other compartments, such as optical detectors, electrodes specifically

in the implementations of test voltages and currents, and closed-loop temperature controllers.

These complex devices permit modification of the fluid by micro channels, the separation of its component by stratified paths, and the detection of its components by electronic part, which are totally complex processes as individually. The main purpose of fabrication of these systems is conducting biological, physical and chemical researches on fluids, tissues and living organisms, such as DNA analysis, organ mimicking, drug toxicity testing, etc.

Organ-on-a-chip technology is the most advanced discovery and performance of a variety of disciplines such as bio engineering, chemical engineering, micro engineering, techniques of mathematical modelling, biology, biochemistry, physiology, medicine, pharmacology fields to mimic living organs in terms of cell-cell interactions, extracellular matrix and extracellular environment, microarchitecture and biochemical functions.

These microfluidic bioreactor systems allow analyzing organ or multi organ functions and interactions by using organ specific cell cultures and microliters of mediums. Thus, the systems make it possible to develop human organs in in vitro models in terms of healthy or diseased ones, investigate fundamental mechanisms of disease etiology and organogenesis, which provide model platform to drug efficiency, toxicity and discovery of active ingredient of medications. Because, current drug-development and disease modelling researches widely rely on preclinical testing and validation protocols, which are not only costly but also time consuming [9], [12], [13], [15], [41].

Before the organs on chips technology, the researches were focused on 2D and 3D cell culture models. They lack complete 3D tissue microarchitecture that cause degradation of physiological accuracy of cell cultures. On the other hand, organ-on-a-chip technology has introduced an innovative path to construct in vitro models with organ and tissue specific microenvironments, rebuilding microarchitecture of tissues, tissue–tissue and organ-tissue interactions and interfaces, biochemical reactions and signaling functions, and spatiotemporal chemical gradients [21], [22].

Therefore, a unique organ-on-a-chip platform was developed and fabricated that was composed of PMMA in this study. GelMA - alginate with four different proportions were produced by utilizing 3D bio-printer. Those were fabricated in order to emulate tissue scaffold on organ-on-a-chip. Scaffolds were essential to provide

suitable adhesion zone for cells above organ-on-a-chip platform. They were placed on both Petri dish and organ chip platform to make comparison. Afterwards, mouse fibroblast cells (3T3) were introduced to both system and cell viability tests were executed by using confocal microscopy. Thus, the study has aimed to fabricate a unique and effective organ-on-a-chip platform and prove the supremacy of organ-on-a-chip against conventional cell culture platform that is mostly used one, Petri dish.

2. FABRICATION OF THE CHIP SYSTEM

The primary objective of the study was developing an organ platform that oriented to human skin. Because, the skin is commonly required in the studies of development of cosmetics. The mentioned products must be trialed on a living if there is any harmful or unexpected effect before put on the market. Skin is becoming the most important element of these studies since most of the cosmetics are relevant to human skin such as creams, perfumes, and lipsticks. Moreover, replacing or repairing the human skin is one of the most needed treatment, because frequent incidents of fires on houses, factories and forests or similar injuries cause dramatic devastation on human skin firstly.

Therefore, first step of the research was the fabrication of the organs on a chip platform, since it would serve as the proper platform in order to produce a suitable environment for mimicking the human skin. In order to achieve this goal, the literature was scanned for previous organs-on-chip structures and specifically for skin-on-a chip models in order to design a unique chip platform [1, 4, 6, 30, 46]. Finally, a genuine chip system was developed by using AutoCAD 2012 modelling program.

Preliminary design of the chip was done by using PowerPoint 2017 program. The chip was designed as 10 layers with 2 mm thickness. One layer served as bottom/top of the chip, three layers was served as bottom layer for cell adhesion and proliferation without involving injection channels and chambers. Six layers were developed as three specialized layers that includes inlet injection channels and reaction chambers and outlet channels. The design was chosen to represent the three different layers of skin, which are epidermis, dermis and hypodermis.

All layers of the chip have 75 mm of length, 50 mm of width. Besides, they contain eight holes with 5 mm length and 5 mm width, which three of the holes localized at the bottom, three of them are at the top, and two of them are at the sides

of the chip for bolt insertion. The distances of the holes were designed as 10 mm for each region (bottom, top, and sides).

Figure 2.1 shows the detailed preliminary design of the chip without injection channels and reaction chambers that was one of the bottoms (or roof) layer of the chip.

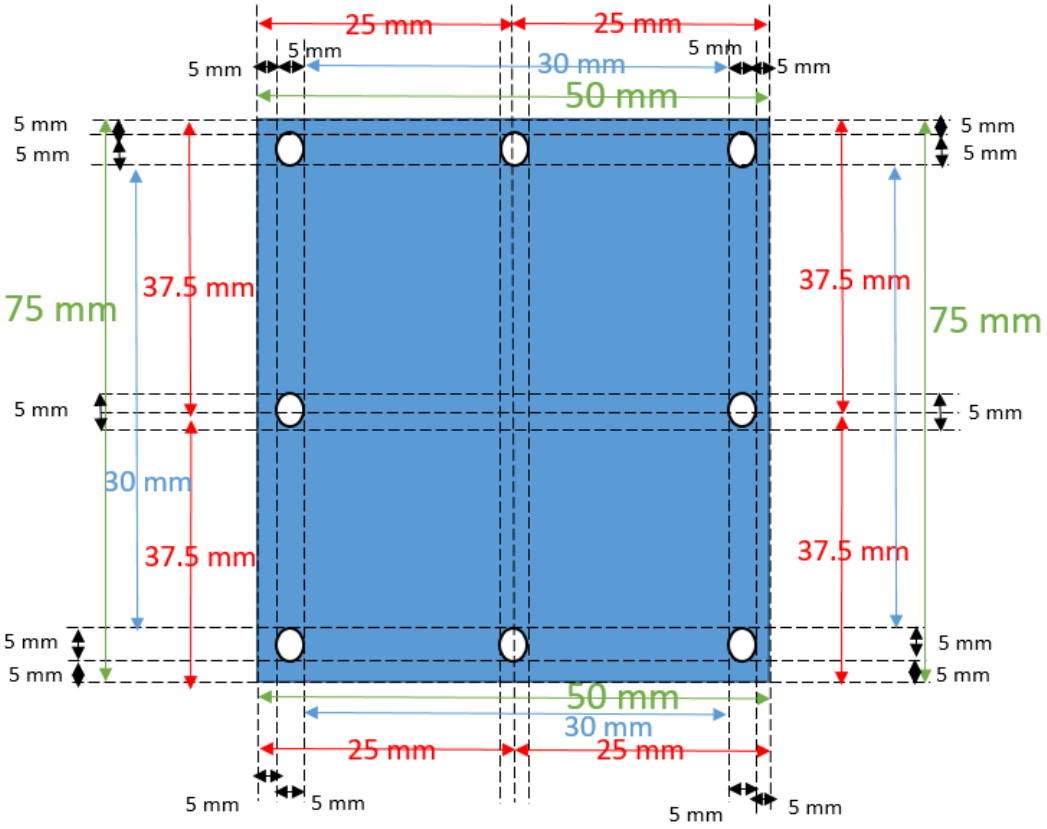

Figure 2.1: Preliminary design of four layers without injection channels and chambers.

Three outlet layers of the chip that were containing injection channels and reaction chambers were designed as following. The outlet channel was designed as an L- shaped structure. The long part was designed as 20 mm in length and 1 mm in width. The small part of the L was designed as 5 mm in length and 2.5 mm in width. 5 mm of the channels were integrated to each other. A final channel that connects the outlet channel to the reaction chamber was designed of 1 mm in length and 0.2 in width. Reaction chambers were developed as balloon shape with 10 mm of diameter and 25 mm of total length. Total volume of the reaction chamber is 662 mm^3. Reaction chamber was calculated by accepting the shape of it as half sphere and triangular prism. Mathematical calculation can be shown as:

The volume of the half sphere: 4 x 3.14 x 5^3 / 6 = 262 mm^3

The volume of the triangular prism: 10 x 20 x 4 / 2 = 400 mm^3

The total volume of the reaction chamber: 262 mm^3 + 400mm^3 = 662 mm^3

The detailed image of outlet layers of the chip was shown in Figure 2.2.

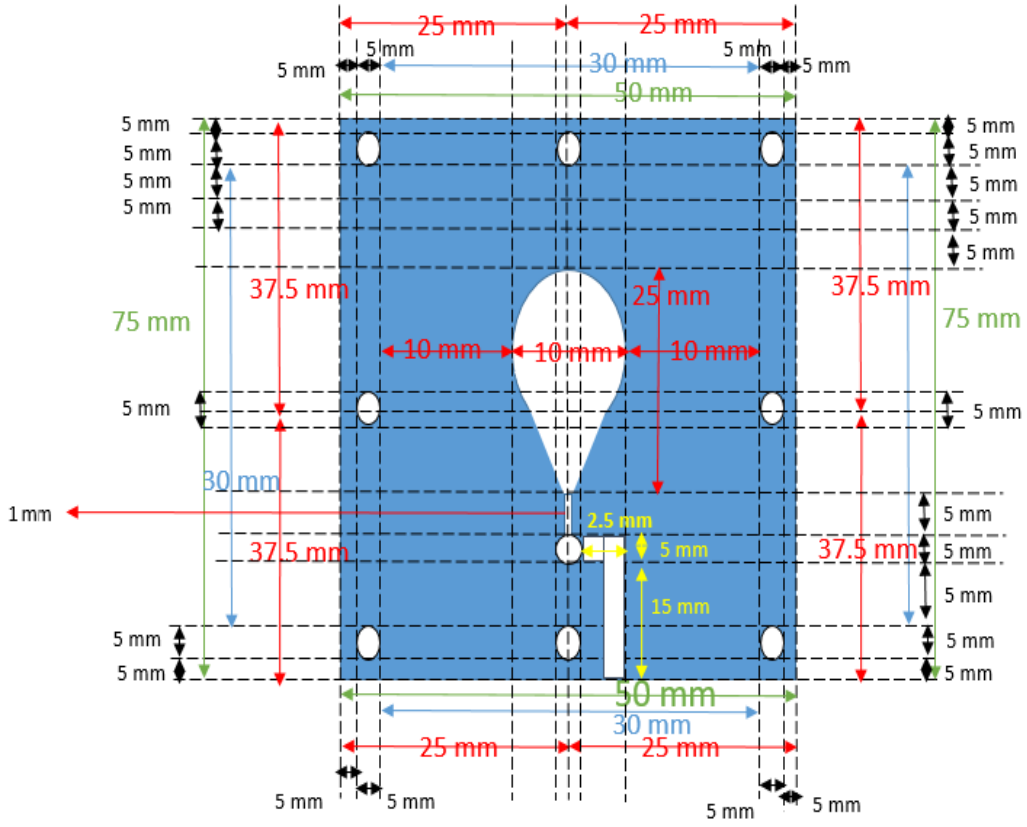

Figure 2.2: The detailed illustration of outlet chambers of the chip.

Three inlet layers of the chip that have connection from cell chambers to injection channels were designed as following. The inlet channel is designed as an L- shaped structure. The long part is designed as 20 mm in length and 1 mm in width. The small part of the L is designed as 5 mm in length and 2.5 mm in width. 5 mm of the channels are integrated to each other. A final channel that connects the outlet channel to the reaction chamber was designed of 1 mm in length and 0.2 in width. Reaction chambers were developed as balloon shape with 10 mm of diameter and 25 mm of total length. The injection channels of the inlet layers were designed as opening the reaction chamber from balloon shape part that was done in order to provide wide range of

injection of medium to reaction chambers and ease spreading. The layers were illustrated in Figure 2.3.

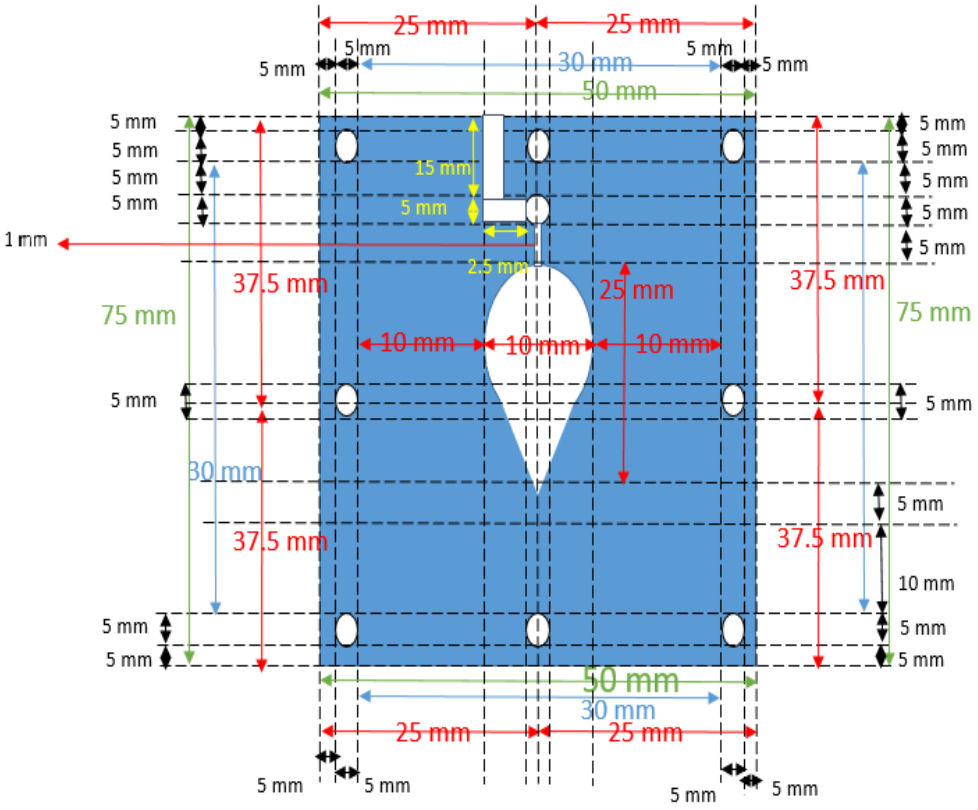

Figure 2.3: The detailed illustration of inlet chambers of the chip.

After the preliminary design, AutoCAD 2012 (Tuna Pleksi Lazer Kesim Sanayi ve Tic. Ltd. Sti.) was used to critical design of the chip. Because the chip is composed of PMMA, laser-etching machine was utilized for fabrication process. Every detail was transferred to sketching. Layers are presented as red for top layers and yellow for interlayers. PMMA was used intentionally, it is one of the most used material for microfluidic and nanofluidic technologies [3].

Because, this thermoplastic has low cost, high transparency. It is also rigid, has a strong impermeability against air, compatible for electronics. and good chemical and mechanical properties compared to PDMS [44]. Furthermore, since it was worked on material for years, there are variety of handling methods [33]. PMMA is strong and tough as physically while it is lightweight. On the other hand, PDMS is a flexible organosilicon material and it is relatively low-cost. Besides, it is transparent and it has

ability to permeability to gases. However, it requires expensive special tools (i.e. soft lithography) to manufacturing process [38] and it also requires clean room.

Additionally, it has weak chemical resistance compared to PMMA. PDMS is closed system when it is fabricated, which means there is no possibility to disintegrate the system. Therefore, PMMA was used as organs on a chip platform material because it was cheap, physically and chemically durable, easy to manufacture, and ability of integration and disintegration after the fabrication process. Figure 2.4 shows the critical design of the chip by utilizing AutoCAD 2012 program.

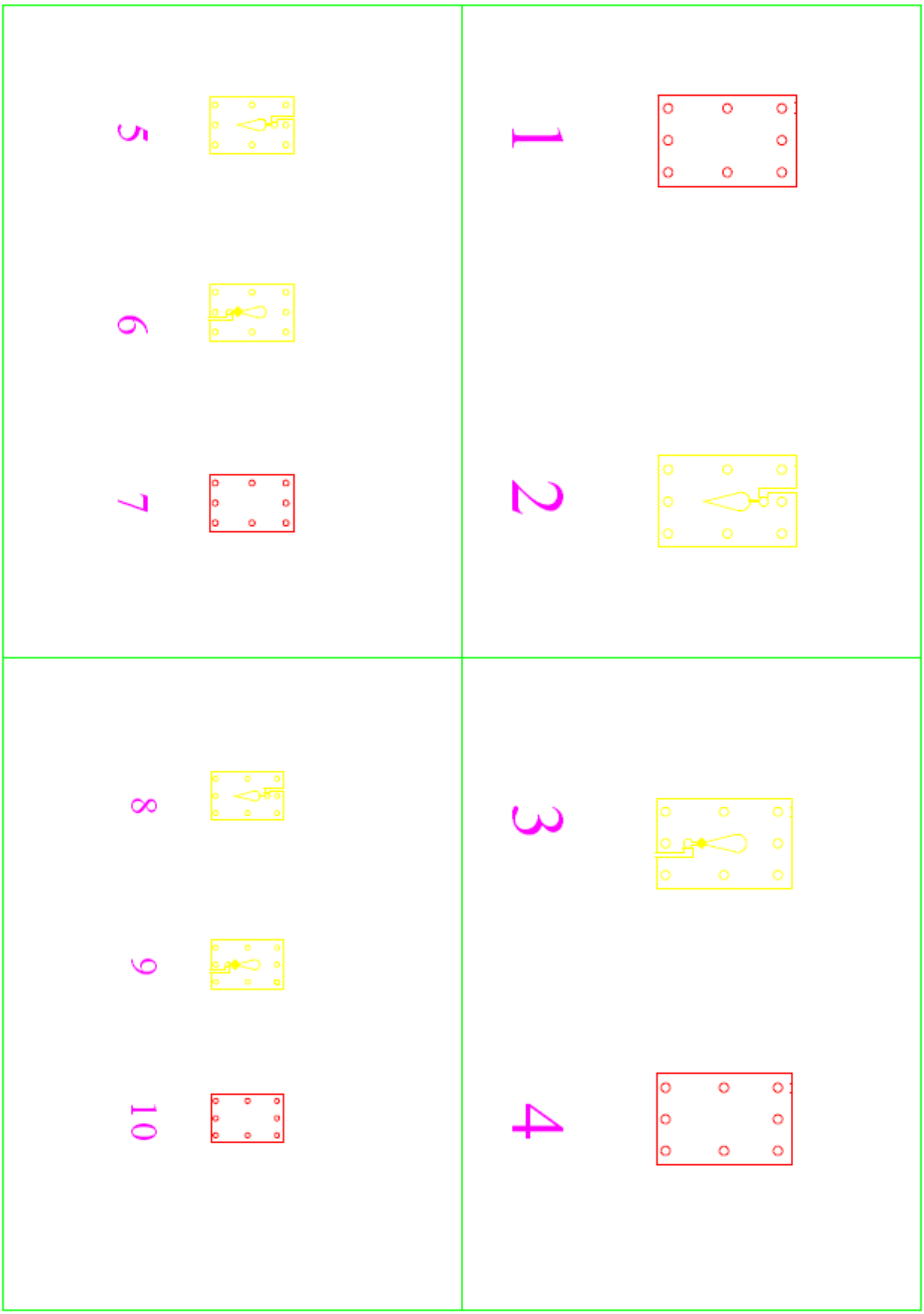

Figure 2.4: The layers of the chip in AutoCAD 2012 design.

Firstly, previously purchased PMMA plate was inserted into the laser-etching machine. The etching machine (Seilaser branded NGRL 1620) was calibrated and then designed AUTOCAD file was initiated. The etching machine has 230-watt, CO_2 laser (Rofin, Germany) with capability of 2049 working hours. Lens is 5 inch and it has 70 mm height. Working area is 2000 mm for X, 1600 mm for Y, and 70 mm for Z axis. Mechanical repletion sensitivity is lower than 0.05 mm, X-Y axis sensitivity is 0.002 mm, and maximum pictorial sensitivity is 1200 dpi. Maximum etching momentum is 20 m/s^2, maximum linear etching momentum is 2000 mm/s, and maximum pictorial speed of Y-axis is 2000 mm/s. It has single-phase etching and three phase chilling property. The laser etching was started to etch the PMMA plate in order to fabricate as the desired shape. However, after the etching process, the selected PMMA structure has burned due to the intensity of the laser beams due to the high density of acrylic presence within the plate. Figure 2.5 presents the PMMA plates after the laser beam application.

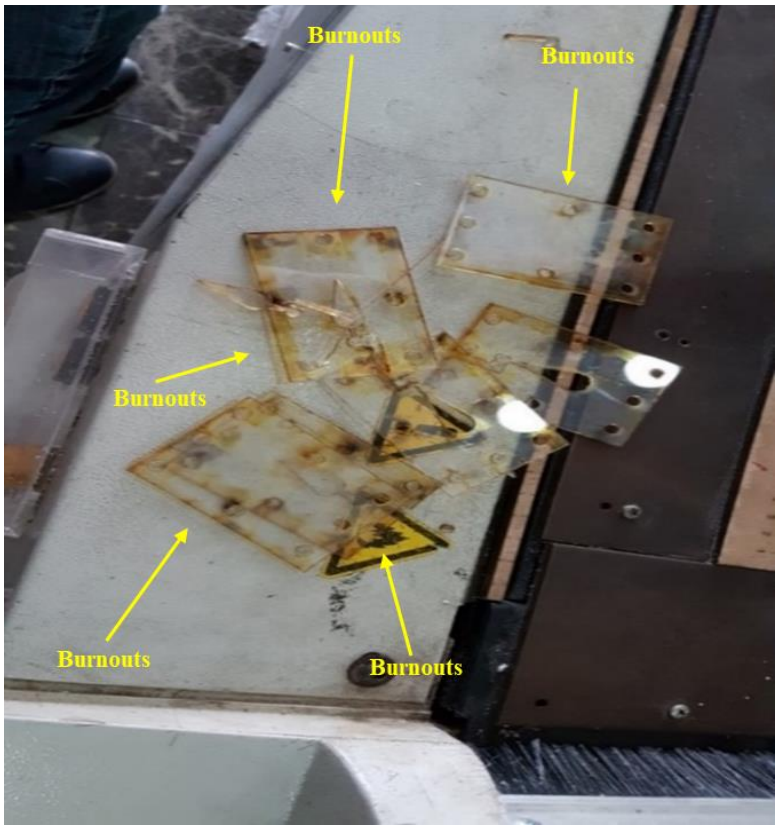

Figure 2.5: Burnout layers of PMMA plate.

Therefore, in order to overcome aforementioned burnout problem, high quality urethane based PMMA plate with protection film was used to give the desired shape. The etching machine successfully cut the layers without causing any darkening or burning, Figure 2.6 shows the etched layers of PMMA plate.

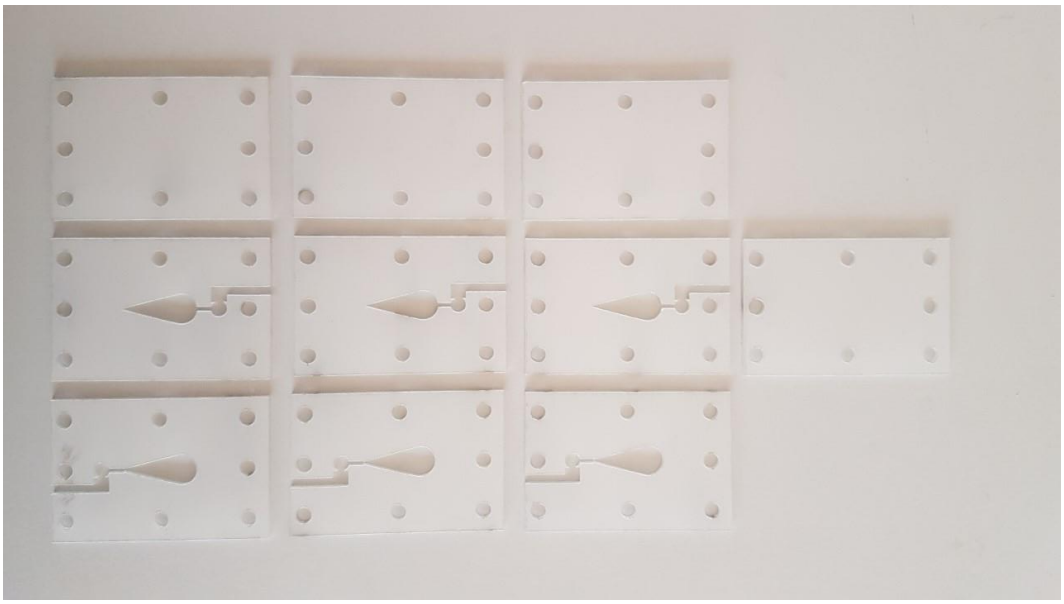

Figure 2.6: The etched image of PMMA layers.

After the successful fabrication, chip layers were examined if there were any signs of manufacturing defect. Then, the chip was stored for further usage. Final aspect of the chip was shown in Figure 2.7.

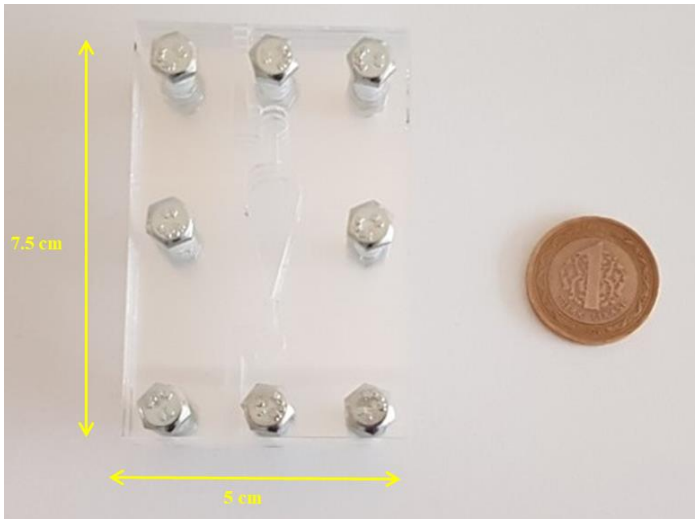

Figure 2.7: The final aspect of the chip with comparison to 1 Turkish Lira.

As it can be seen from Figure 2.7, the chip is visibly small, integration and disintegration of layers of the chip is easy which provides mobility, reproducibility, easy to sterilize, and easy to change the conformation of the system according to the study.

3. BIOMATERIALS FABRICATION AND 3D BIOPRINTING

3.1. Fabrication of GelMA

Gelatin methacrylate is one of the most known and used material in bioengineering and tissue engineering implementations, especially in 3D culture systems, drug delivery and scaffold fabrications. GelMA is a hydrogel that composed of natural and modified components of ECM, which can be photo-polymerized.

Gelatin part not only preserves the natural cell linking motives such as RGD (Arg-Gly-Asp), but also preserves MMP (metalloproteinase) sensitive degradation sites. Addition of methacrylate groups to side groups of gelatins that contain amine results production of a hydrogel, which can be polymerized via using light that was shown in Figure 3.1. Therefore, it was fabricated to be used to fabricate of tissue scaffold, which would be placed in both Petri dish and the microchip system in this study.

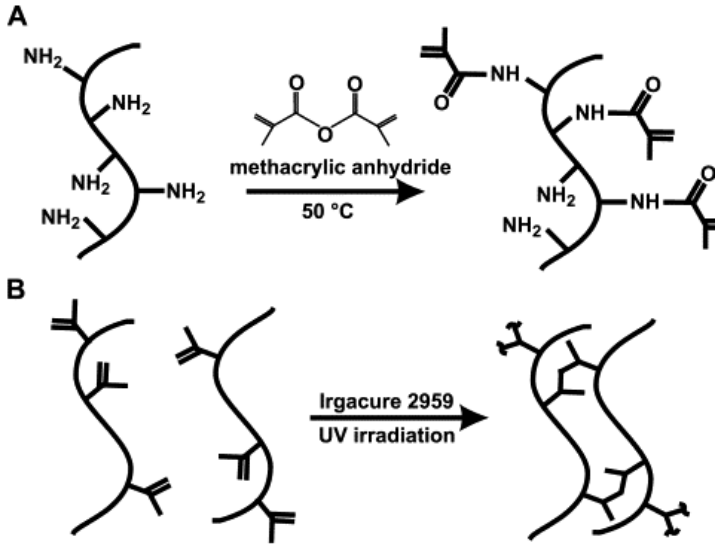

Figure 3.1: A) Constitution of Gelatin and Methacrylic anhydride compound at 50 °C B) Interaction of GelMA hydrogels under the UV light.

10 g of porcine skin (type A) was weighed and transferred Erlenmeyer flask that was sterilized via using 70% of ethyl alcohol. Then, 100 ml of PBS was added to flask and it was mixed. Undissolved mixture was placed on heating plate and mixed at 240 rpm at 50 °C until the gelatin completely melted. The solution was analyzed if there are presences of gelatin granules. After the analysis, no granule was detected, which meant the gelatin fairly melted and a homogeneous solution was achieved. Afterwards, Erlenmeyer flask was coated with aluminum foil in order to protect any kind of light and heat source from the environment.

After the melting of gelatin, 8 ml of Methacrylic Anhydride was slowly and drop by drop added to Erlenmeyer flask by utilizing 1000 µl pipette. The new solution was again mixed at 240 rpm at 50 °C in magnetic mixer for 2 hours. The flask was coated with aluminum foil and the procedure was proceeded in a safe place since evaporation of Methacrylic Anhydride has dangerously toxic effect.

100 ml of sterile DPBS was measured, added in Erlenmeyer flask, and it was heated at 50 °C. After that, heated DPBS was used to dilute the mixture of Gelatin-Methacrylic Anhydride, final volume of the mixture raised to 200 ml. The new mixture was mixed in magnetic mixture right 10 minutes at 50 °C. This procedure was conducted in order to stop the reaction being realized between Gelatin and Methacrylic Anhydride.

Dialysis membranes also known as Visking tubes (Spectro/Por molecularporous membrane tubing, MWCO 12-14,000, Fisher Scientific) was prepared cutting in the length of 30 cm and they were dipped into distilled water in order to soften the materials. An edge of the membranes was tied, then distilled water was poured from open mouth to membrane in order to detect if there was leakage on the tied edge. Diluted GelMA was transferred to membranes by using funnels.

The opened mouths of the membranes were tied exactly the same as first tied edges without leaving a bit space. Because, the leaving space provides enough area to easy movement of distilled water and in and out motion in membrane during the dialysis process, which results much fruitful output. After the last checking for any sign of leakage, the membranes were placed plastic beakers that is filled with 5L of distilled water. Dialysis membranes were dialyzed in 5L of distilled water at 500 rpm and at 40 °C for 7 days. Distilled water in the beakers was replaced with the new ones twice a day and the membranes were turned upside-down five-six times a day.

Thus, Methacrylic Anhydride residues that were not reacted in the system could be easily removed.

200 ml of ultra-pure water (same amount with the gel in the membranes) was added to Erlenmeyer flask. Then, dialyzed GelMA was added on distilled water and the solution was heated at 40 °C and 15 minutes. Eleven pieces of Falcon tubes were prepared for GelMA storage. Diluted GelMA was filtered by using coffee filter in order to dispose of remaining pollutions in the liquid.

Afterwards, Express Plus (0.22 μm) Millipore sterile vacuum filtration pot was utilized for implementing more detailed filtration. These steps were executed as soon as possible in order to maintain the heat of the liquid at 40 °C. Sterilized polymers that completed the phases of filtration were transferred to Falcon tubes (50 ml) about 25-30 ml and they were stored at -80 °C horizontally for 5 days. Horizontal placement was implemented for providing convenience for following step drying process.

Frozen GelMA at -80 °C were lyophilized. Firstly, the covers of falcon tubes were removed, and then they were closed with Kimwips by using rubber tires. They were awaited in freeze drying machine for 4 days.

The dried GelMA was stored at -20 °C for further implementations. The ultimate state of GelMA was shown in Figure 3.2.

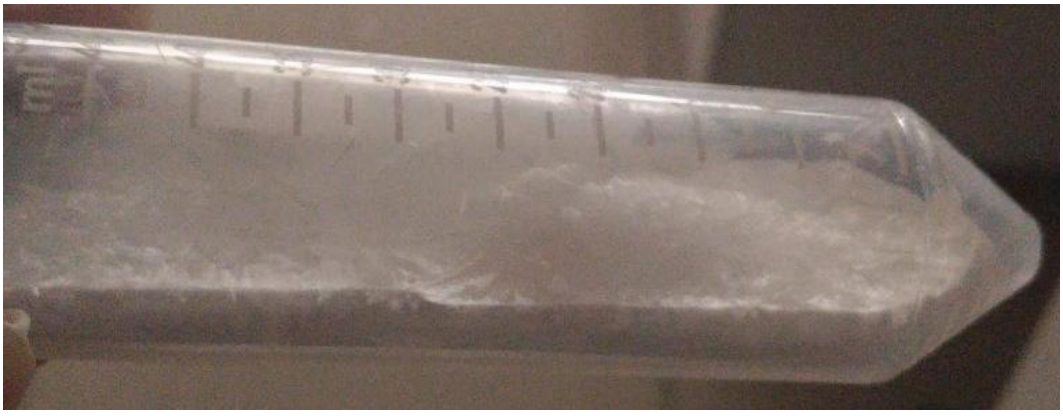

Figure 3.2: Final aspect of GelMA in foam-like structure.

3.2. Fabrication of GelMA - Alginate Solution

In this study, GelMA and alginate mixture was used as tissue scaffold material. As abovementioned in section 3.1 GelMA is a preferable material in tissue engineering applications. Because, it has ability to offer suitable environment for the cells to

proliferate, migrate, and even differentiate [31]. Besides, it shows high biocompatibility thank to its gelatin content, shows good mechanical strength, and ability to constitute cross-links thanks to its methacryloyl content [5]. However, it is challenging to use GelMA alone since it is expensive material, insufficient shape fidelity, limited rigidity, and it lacks viscous composition especially for printing procedures [42]. On the other hand, alginate is a natural polymer (anionic polysaccharide) that is derived from brown seaweeds (mostly) shows high biocompatibility, low toxicity and fast gelation ability [5].

However, alginate has almost no bioactivity that causes minimal cellular adhesion. It directs researches to use additional materials. Therefore, GelMA and alginate mixture is used in order to develop a fully biocompatible and mechanically tough material by compensating of cons of each other. Alginate provides a suitable template and mechanical support for the scaffold, act as a stabilizer and GelMA provides high bioactivity, high cellular interactions, and cross-linking enhancer.

In this study, previously fabricated GelMA and previously purchased alginate (E401, ALFASOL, 100 g) were used to produce biomaterial. It was produced in order to be used in 3D bio-printer for printing the scaffold, which shall be assigned as a structure in both Petri dish and organs on a chip platform to provide suitable platform for adhesion and proliferation processes of the cells.

Firstly, four different solutions were prepared as:

10% GelMA (1 g) + 7% alginate (0.7 g) + 0.1% Irgacure (0.01 g) + 10 ml PBS,

7% GelMA (0.7 g) + 5% alginate (0.5 g) + 0.1% Irgacure (0.01 g) + 10 ml PBS,

7% GelMA (0.7 g) + 4% alginate (0.4 g) + 0.1% Irgacure (0.01 g) + 10 ml PBS,

5% GelMA (0.5 g) + 4% alginate (0.4 g) + 0.1% Irgacure (0.01 g) + 10 ml PBS,

Those four proportions of the mixtures were determined by literature researching [8], [47], [49]. As mentioned before, increasing concentration of GelMA provides more cross-linking possibility. Differently, alginate can be cross-linked fast and irreversibly, which makes the printed structure stabile. However, excess amount of alginate causes undesired viscosity, which makes bio printing process challenging. On the other hand, Irgacure was used in the mixture. Because, it is a radical photo initiator that produces reactants when UV light is applied. It is especially preferable for acrylate

resin. Therefore, it realizes and accelerates the cross-linking process of GelMA when it is exposed to UV light.

GelMA (previously prepared) was weighed as 1 g in precision scales, and then was transferred into falcon tube (50 ml). Sodium alginate (purchased) was weighed as 0.7 g in precision scales and was transferred into the same falcon tube.

Finally, 10 ml of PBS was added to falcon tube and it was mixed by using vortex mixer to achieve desired consistence. Finally, the tube was placed in water-bath (Thermomac, WB22) at 37 °C. Same process was conducted for the other three different GelMA - alginate ratios (7%-5%, 7%-4%, 5%-4%) with 10 ml of PBS. Then, four different solution with different densities were stored at 4 °C in refrigerator for bio-printing process.

3.3. Fabrication of Tissue Scaffold

After the production of biomaterials that consists of GelMA and Sodium Alginate, time has come to fabrication of tissue scaffold for both Petri dish and organs on a chip platform. The four different mixtures of GelMA and Sodium Alginate (10%-7%, 7%-5%, 7%-4%, 5%-4%) was loaded to injection barrel (Nordson EFD, Clear HiTemp Tapered) with stemmed tip cap (Nordson EFD) of the bio-printer via using spatula spoon (BOROX stainless steel).

First, the bio-printer (Axolotl Biosystems, axodual) was opened, and then routine calibration was done by measuring the movement of syringe millimeter by millimeter through the printing table in X-axis, Y-axis, and Z-axis. That was executed in order to prevent any non-precise printing and out of range (Petri dishes) printing. After the calibration, height of the layers was set to 100 μm and then the diameter of the scaffold was set as 1 cm (minimum).

For layers and perimeters, layer height was selected as 0.1 mm. It is essential to fabricate the surfaces smoothly and precisely. Choosing the layer height lower provides curves and angles more precisely. Besides, since it would place onto organs on a chip and the Petri dish, total height of the scaffold must not be high. Perimeters of the vertical shells of the bio-printer was selected as 1 (minimum). Because, increasing the perimeter causes thicker walls of printed material that is not necessary for this study.

Secondly, printing density of the scaffold was set as 3%. It determines the density of the materials. For instance, if the fill density is set to 100%, the material will be completely solid, there will be no space inside the shell of the material. In contrast, if the fill density is set to 0%, the inside of the shell of the material will be empty, which become lighter. Therefore, low printing density was chosen. Because, high density requires high amount of material and it was not necessary in this study. Fill pattern was selected as rectilinear, it provides desired rigidity in total and surface are to cell adhesion and proliferation, and easy to print.

Finally, printing speed was selected. The speed of one circling around a layer was set to 60 mm/s. It was selected to provide healthy printing procedure without causing disfigure the pattern of the scaffold and preventing congestion of solution in the injection syringe. No acceleration values were inserted the printing calibration because of abovementioned reasons. Any other calibration and arrangement of other speed parameters of the system was not executed. 10%-7% GelMA - alginate containing syringe was integrated to bio-printer's injection channel in order to start printing process, which was shown in Figure 3.3.

Figure 3.3: The syringe with orange head loaded bio-printer.

Structure of scaffold that was about to be printed was selected as circular mold (with rectilinear infill) by using Repetier software (Repetier Host V2.1.3) that was integrated interface to bio-printer, which was shown in Figure 3.4. That specific shape

was preferred, since it was easy to print and the experiment has not required any specific condition but cell adhesion and proliferation. Estimated printing time is resulted as 1 minute, since the scaffold is small and in basic shape. Layer count is determined as 10 layers.

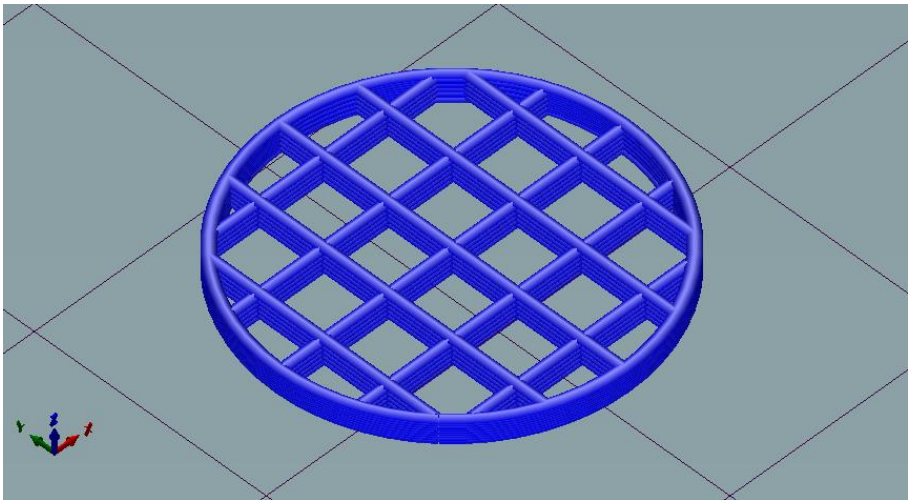

Figure 3.4: The structure of the scaffold to be printed.

Then, Petri dish (90 mm × 15 mm, glass) was placed on the printing table. Printing pressure was set to 36.3 psi. First, stemmed tip cap (Nordson EFD) was used with injection barrel (Nordson EFD, Clear HiTemp Tapered), which is durable up to 125 °C and 87 psi. However, the pressure was 36.3 psi and it was insufficient to print a mixture that contains viscous and dense solution; alginate which was at 10% of total volume. In addition, barrel cap width was massive that was excessive for printing a viscous liquid, the printing could not be executed. Literally, there was no material on the surface of the Petri dish. Thus, stemmed tip cap was removed and precision tip (Nordson EFD, type 21 GA, 020X.5 Purple 50PC) was utilized in order to provide essential printing precision.

In addition, printing pressure was raised up to 68 psi (maximum value of the bio printer). It was appeared that due to the presence of high percentage of the alginate, the mixture became so viscous. Therefore, in order to reduce the viscosity, the printing speed was set to 25 mm/s, it is optimum speed for small materials to be printed in terms of diameter and shape. Because, speed and printing precision are inversely proportional. For instance, the speed is increased, the printing quality become superficial in order to compensate the printing time. After the necessary regulations,

the precision tip was located right above the Petri dish and then fabrication of scaffold has initiated.

Figure 3.5 presents the tissue scaffold achieved by 10% - 7% GelMA Sodium Alginate Mixture. Finally, printed scaffold was subjugated to UV light (365 nm) for 100 seconds in order to provide hardening of the structure by initiating covalent cross-linking of the mixture.

Six pieces of scaffold with 10% GelMA-7% Sodium Alginate mixture were fabricated and hardened with same procedure, then they were stored in refrigerator at 4 °C.

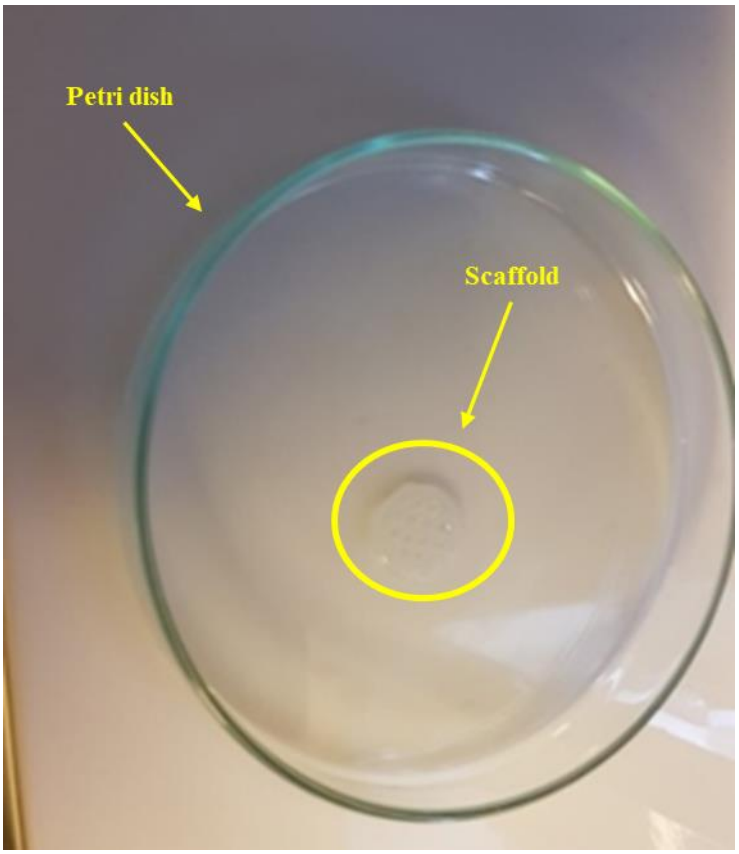

Figure 3.5: The printed scaffold with 10% GelMA-7% Sodium Alginate mixture.

Second attempt were done with 7% - 5% GelMA and Sodium Alginate mixture. 7%-5% GelMA and Sodium Alginate mixture containing syringe was replaced with former one (10%-7%) into the injection barrel. Petri dish (150 mm × 25 mm, glass) was again placed onto the printing table. Printing pressure was set to 36 psi since the alginate proportion was lower than the former one. Printing speed was adjusted to 25 mm/s. Afterwards, quick calibration was executed by moving the nozzle to X, Y, and

Z axis in order to maintain the precision of printing and prevent post-deterioration in the system. Printer was started and tissue scaffold was fabricated. Later, it was subjugated to UV light for 100 seconds. In total, six pieces of 7%-5% GelMA and Sodium Alginate containing tissue scaffold were fabricated. Figure 3.6 shows an example of the printed scaffold.

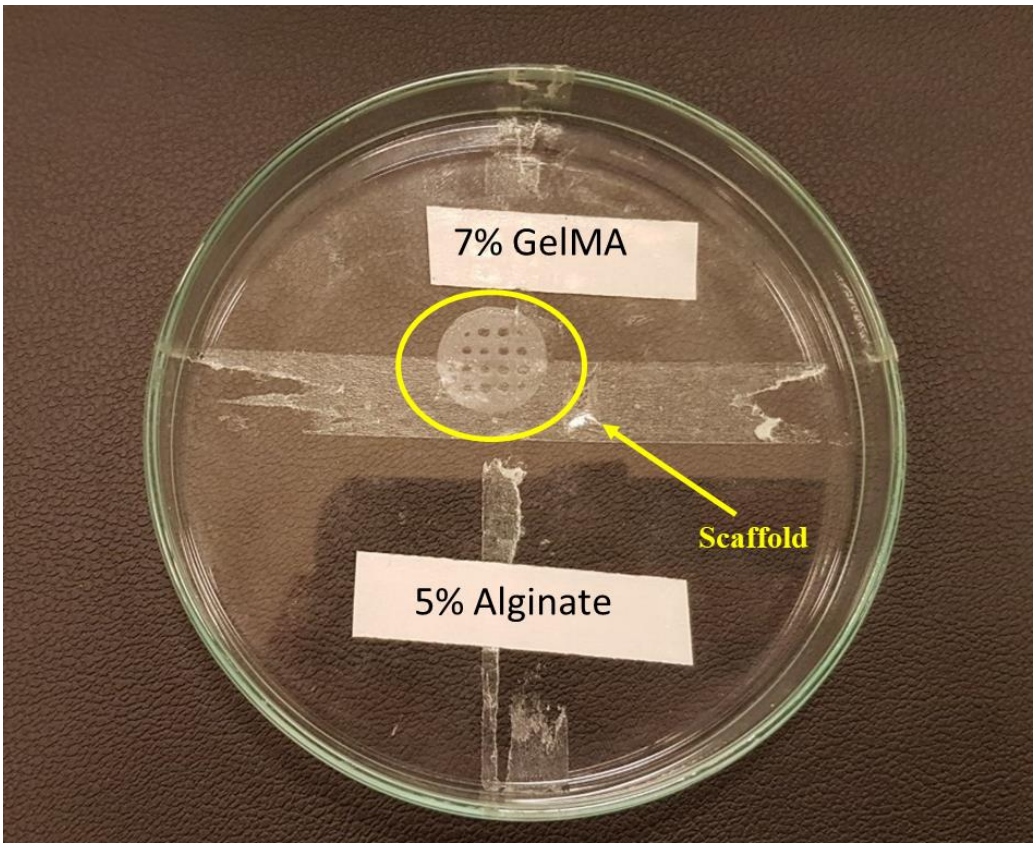

Figure 3.6: The printed scaffold with 7% GelMA-5% Sodium Alginate mixture.

However, fabrication of the mixture of GelMA and Sodium Alginate with 7%-4% and 5%-4% were failed. The given pressure was only 18 psi. Because when the previous pressures were adjusted (36 or 68 psi) to print the scaffold, the mixture was totally disintegrated and printing in a desired shape was not observed. After the several trials to adjust pressure in required level, the pressure was determined as 18 psi. Lower level of the adjusted pressure (18 psi) was not able to inject the mixture, the pressure was insufficient particularly.

As it was shown in Figure 3.7 and Figure 3.8, there were no rectilinear structures in the scaffold and the general architectures were so soft and formless. That was appeared because of amount of GelMA and alginate in the system. Because, amount

of GelMA is crucial for initiation of cross-linking process with photo-initiator, it has poor mechanical properties in physiological temperature, low ability to extrude alone and unstable on the other hand. The essential amount of alginate is crucial for providing gelation process, indicating satisfactory stability and integrity. It lacks bioactivity for cells to adhere and proliferate.

Therefore, the deficient amount of alginate caused fluidic output of printing. In Figure 3.7 deformed structure of the scaffold can be observed, rectilinear architecture was absent and the composition of the mixture was so soft. In Figure 3.8 rectilinear form is completely absent and printed mixture exhibits a droplet form.

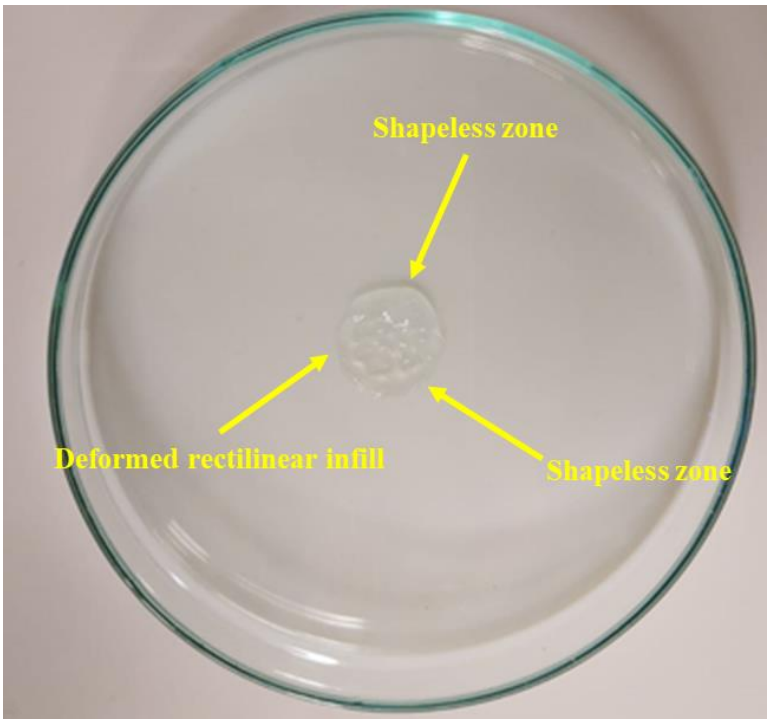

Figure 3.7: The failed fabrication of 7%-4% GelMA - alginate scaffold.

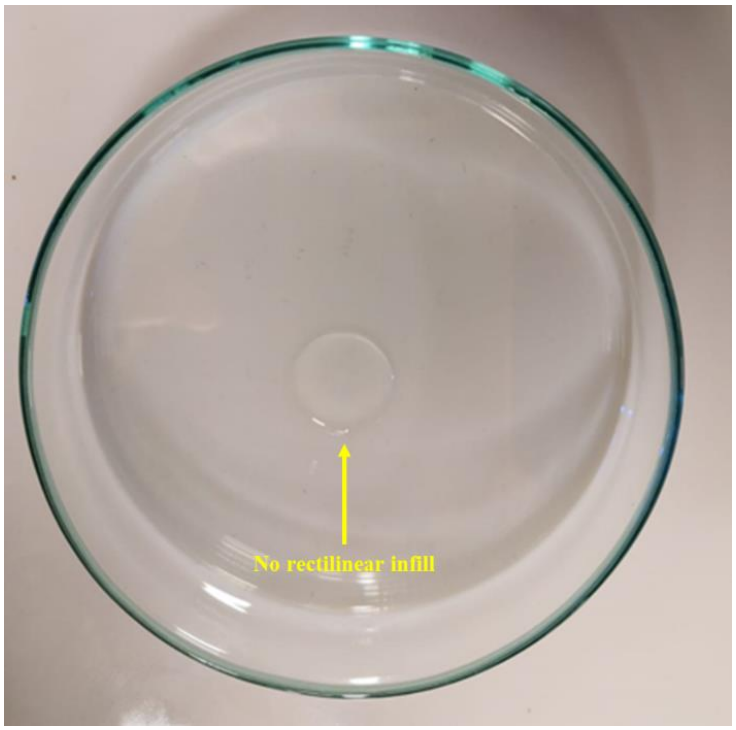

Figure 3.8: The failed fabrication of 5%-4% GelMA - alginate scaffold.

Finally, twelve pieces of GelMA – Alginate containing scaffold were successfully printed. Six pieces of them were represented by GelMA – Alginate in the ratio of 10%-7%, the remaining six pieces were represented in the ratio of 7%-5%.

4. CELL CULTURE AND CELL VIABILITY

4.1. Cell Culture

In order to achieve cell culture both on Petri dishes and organs on a chip platform, first, mouse fibroblast cells (3T3) were obtained in T25 Flask (Thermo, Fisher Scientific). After the fibroblast cells were acquired, the cells were grown in DMEM (Dulbecco's Modified Eagle's Medium, SEROX) culture containing 10% FBS and 1% penicillin / streptomycin (SEROX) in an atmosphere of 5% CO_2 at 37 °C. When the cells reached 80% fullness, the cells were passaged by adding 2.5 ml of a 0.25% Trypsin-EDTA to flask. After that, it was incubated about 45 seconds at room temperature and gently shaken to accelerate disassociation of the cells. Same amount of (2.5 ml) medium was added to the flask after 45 seconds in order to neutralize pH

balance of the cell environment. Then, the cells were transferred to the Falcon tube (50 ml) and centrifuged (nüve, NF 400R) at 1000 rpm for 5 minutes. The cells precipitate to the bottom of the Falcon as cell pellet, the supernatant (dead cells and the medium) were removed and then 1 ml of cell medium was added to the Falcon to solve the cells.

10 µl of cell suspension was taken and transferred into Thoma lamina by using micropipette as a drop. Then, the cell counts were executed under the light microscope to detect cell number that was shown in Figure 4.1.

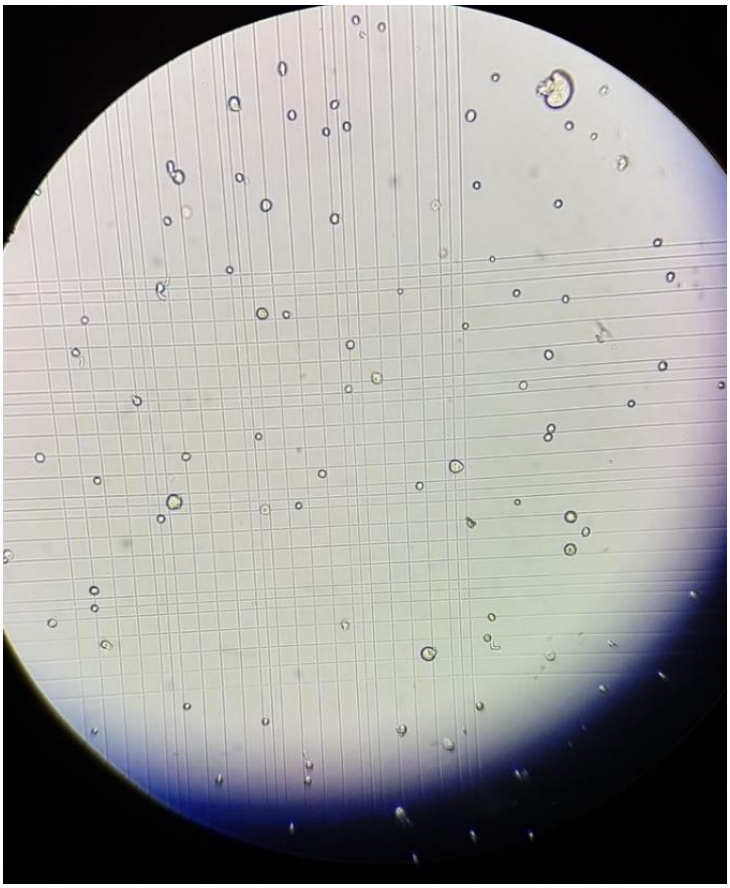

Figure 4.1: The cells in Thoma lamina for cell counting.

Finally, optimal cell amount was detected as $4x10^5$. In the meantime, all compartments of the organs on a chip platform that were 8 bolts, 8 loaf, 10 PMMA layers, needle, injection pipe and the glass Petri were placed into biosafety cabinet (Esco, class 2). They were exposed to UV light at 254 nm wavelength for 15 minutes, which is optimal wavelength and elapse time for germicidal operation. Afterwards, the density with $4x10^5$ cell/Petri containing cell-medium solution was transferred into the glass Petri that contained 7%-5% GelMA - alginate mixture scaffold. The Petri was

placed into the incubation tank (nüve, EC 160) at 37 °C with 5% CO_2. Sterilized organs on a chip platform was superposed layer by layer as being plane layer, outlet layer, and the inlet layer until the 8th layer. 9th layer was superposed after the tissue scaffold was inserted onto the 8th layer. 9th layer is the layer of the cell chamber with an outlet channel.

The scaffold was placed on 8th layer by using mini spatula, injection tube integrated into inlet channel of the same layer and then fibroblast cells were transferred into the scaffold in the chip by using micropipette with same proportion ($4x10^5$ cell/Petri). Finally, 9th layer that contains an outlet channel and 10th layer as the top layer of the organs on a chip platform was integrated and all of the layers was tighten via inserting the bolts and loafs by using spanner. The location of the holes was determined during the preliminary design and fabricated during critical design. Figure 4.2 presents a fully integrated organs on a chip platform.

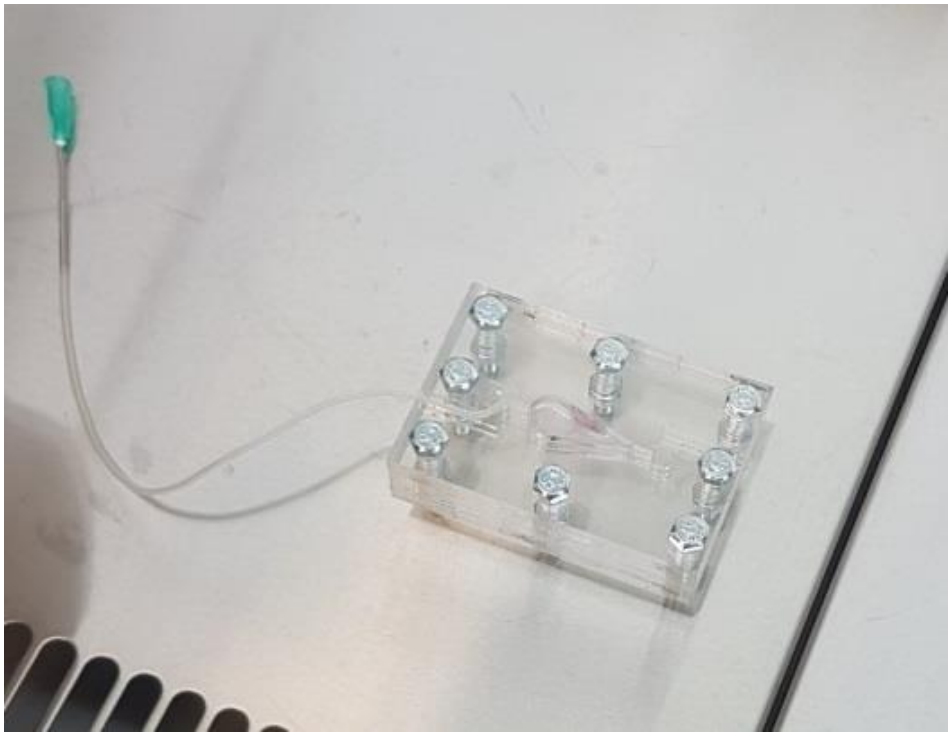

Figure 4.2: Fully integrated skin chip system with injection-ready apparatuses.

In the end, the needle that were connected to the injection tube was replaced on 50 ml injector (set inject), which was loaded 50 ml of growth medium. The injector was placed on syringe pump (Harvard Apparatus, Pump 11 Elite). The calibration of the syringe pump was set by determining the diameter of the injector and the velocity

of flow of the growth medium was adjusted as 1 ml/h. The syringe pump was cleaned with 70% ethanol solution. Syringe pump, the chip system, and the Petri dish were placed into incubator tank for 24 hours until the imagining process, which was shown in Figure 4.3.

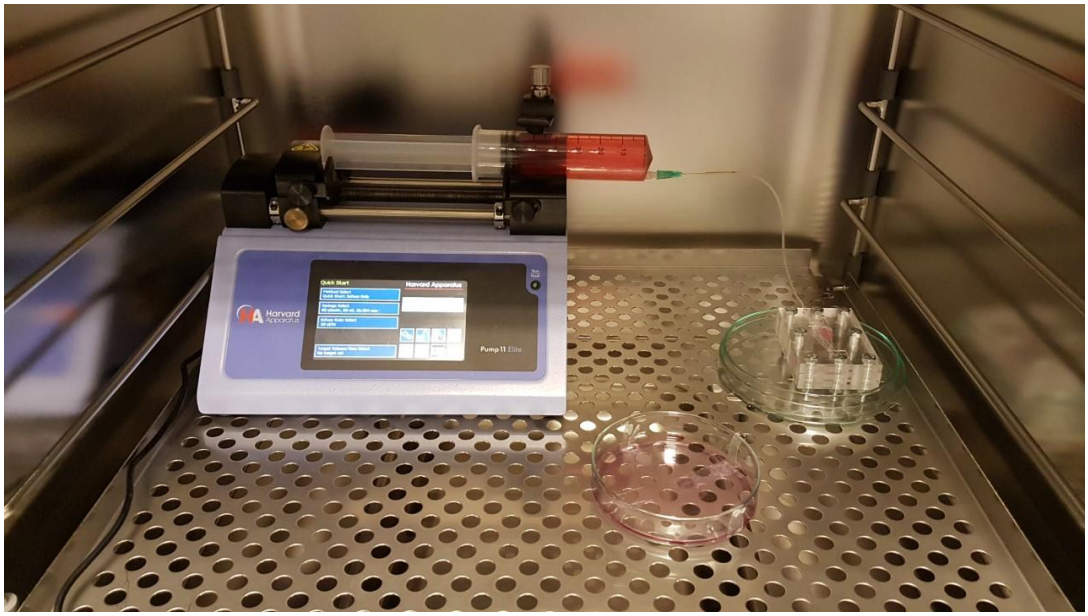

Figure 4.3: The last statuses of both systems, before the initiation of the incubation process.

In the second experiment, GelMA – Alginate containing mixture in the ratio of 10% - 7%. First, the scaffold that was printed onto the glass Petri dish were disassociated in order to transfer the scaffold from glass Petri to organs on a chip. PBS solution was utilized for disassociation process. It was poured into glass Petri until it covered the surface, then the Petri dish was placed in drying oven machine at 37 °C in order to accelerate disassociation. This procedure administered the disassociation of the scaffold from the surface of the Petri.

In the meanwhile, all of the experiment materials that are composed of bolts, loafs, PMMA layers, injection needle, injection pipe and the Petri were placed in biosafety cabinet and they were exposed to UV light (254 nm wavelength). Then, the scaffold was transferred to 8^{th} layer of the organ-on-a-chip gently by utilizing mini spatula. 8^{th} layer served as the reaction chamber with inlet channel, which was only suitable layer for the scaffold placement. Concurrently, mouse fibroblast cells that were in T75 flask were growing in DMEM that contained 10% FBS and 1% penicillin

/ streptomycin. It was in incubator in an atmosphere of 5% CO_2 at 37 °C. Passaging of the cells and transfer from flask to organ-on-a-chip and the Petri dish were conducted at the same time. The fullness of the cells in T75 flask was detected above 85%.

Hence, 2.5 ml of a 0.25% Trypsin-EDTA was added to T75 flask. It was incubated nearly a minute at room temperature. The flask was gently shaken toward X and Y axis in order to advance the process of disassociation of the cells from the surface of the Petri dish. After a while, 2.5 ml of DMEM was added to the flask, which equilibrates the pH of the cell environment. The solution (contains cells, DMEM, and Trypsin-EDTA) was transferred to the Falcon tube. The falcon tube was centrifuged at 1000 rpm for 5 minutes. The mouse fibroblast cells have positioned at the bottom of the Falcon, the remaining solution (supernatant) was disposed.

Then, the cells were solved in the Falcon tube by addition of 1ml of cell medium. 10 µl of cell suspension was taken by using micropipette and dropped onto Thoma lamina. That amount was drawn into micropipette intentionally in order to conduct the experiment with same values as the former one. After the calculating the number of cells in the Thoma lamina, the optimal cell amount was detected as $4x10^5$. Organs on a chip was constructed by integrating the layers from 1^{st} to 8^{th} layer and then the scaffold was placed on reaction chamber.

Finally, $4x10^5$ cell/Petri was drawn into the micro pipette and it was transferred onto the scaffolds in the ratio of 10% - 7% GelMA - alginate that were placed on organs on a chip's 8^{th} layer and the Petri dish. Then, the 9^{th} and 10^{th} layers of organs on a chip was integrated the remaining system by using bolts and loafs. The both systems were placed into incubation tank in an atmosphere of 5% CO_2 at 37 °C. Injector (set inject, 50ml), injector needle, syringe pump, and injection pipe were sterilized by 70% ethanol. Injector with needle was inserted on syringe pump, and the diameter calibration was selected from injector diameter screen.

The flow velocity of the pressure of the syringe pump was adjusted as 1 ml/h. Finally, an end of the injection pipe was connected to inlet channel of organ-on-a-chip (8^{th} layer), the other end was connected to injector needle and then syringe pump was initiated. Figure 4.4 shows the transfer process of the cells from micro pipette to organ-on-a-chip system. The determining of the total volume in the both systems ($4x10^5$ cells) was calculated as:

The volume of the big square of Hemocytometer = Depth x Area

The volume = 0.1 mm x $1mm^2$ = 0.1 mm^3 = 0.1 µl

20 (counted cells) x 1000 / 0.1 = $2x10^5$ in a ml

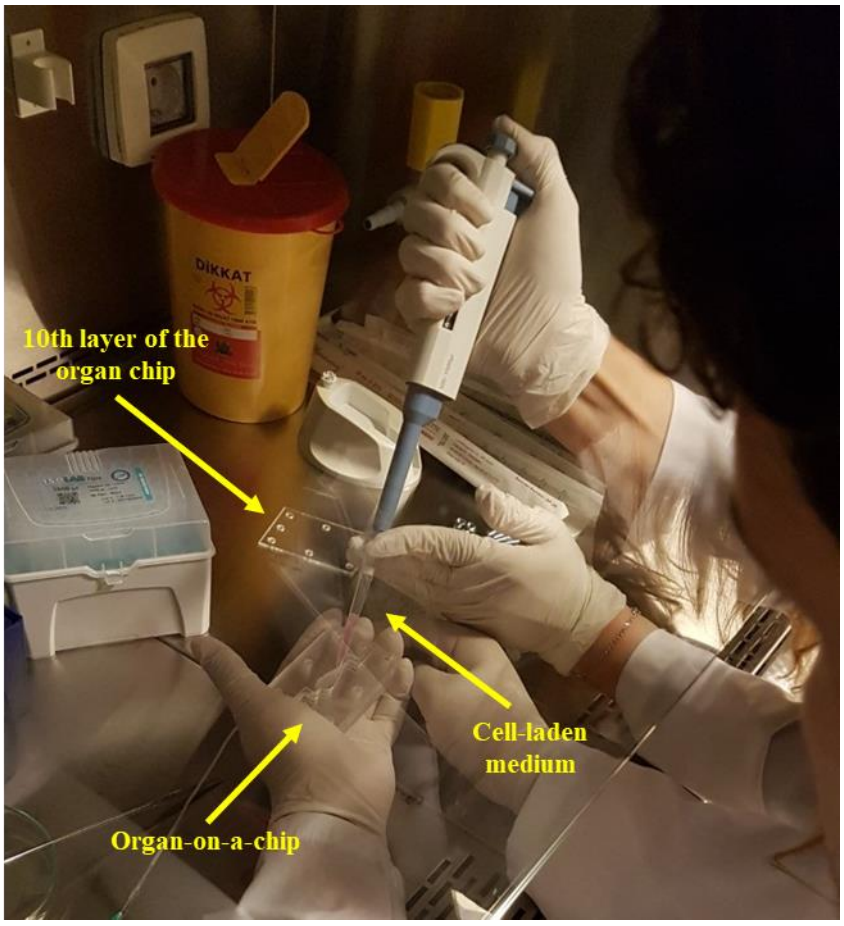

Figure 4.4: Fibroblast cells transfer process to the chip system via using micropipette.

4.2. Cell Viability Tests

As the beginning of the cell viability tests, the scaffold that contains 7%-5% GelMA - alginate solution was analyzed.

The imagining process was conducted by utilizing confocal microscopy (ZEISS LSM 880, AxioObserver). As the beginning, the chip was removed from injector pump by removing the needle from the injector, then the leaked medium, which was coming from outlet part was cleaned and placed on imagining field attentively.

Since any kind of dyeing chemical was not applied on cells neither in the chip nor in the Petri during the process of the cell culture, no colorful luminescence used.

Only PMT was applied during the process of the confocal microscopy imagining. After the essential adjustments of the confocal microscopy, first day images were taken. The organs on a chip images were taken primarily; the Petri was taken secondarily. First day images were taken after 24 hours of incubation period.

Then the chip and the Petri were placed in incubator, the chip was integrated to injector pump until second image-taking process. The image takin process was conducted as selecting three different zones randomly, that was executed to be able to make statistical analysis. First, the present amount of cell in a μm^2 was calculated. The calculation was executed as:

The total volume of the chamber: $6x10^{11}\ \mu m^3$

The number of cells in ml: $4x10^5$

The cells should be present in μm^3: $4x10^5 / 6x10^{11} = 6x10^{-7}$ cells

Thus, the number of the cells in images was found as 40. The first day images were taken by utilizing confocal microscopy. Determination of alive and death cells was executed by analyzing the shapes and the colors of the cells. Since the cells were cultured after the placement of the scaffold onto the platforms, none of dying techniques was used. Therefore, if there was any serious obscuration in the cell, which is the precursor of cell lysis, those cells were counted as dead. In addition, if there was any deterioration or necrosis in the cell, those were counted as dead. On the other hand, smooth circular shaped cells and the cells that show obstruction a bit, those cells were counted as alive. The alive-dead cell counting was calculated via using the equation:

R (%) = alive cells x 100 / total cells

The alive cells were counted as 32 and the dead cells were counted as 7 of total 39 cells, which meant 82% of the adherent cells was alive and the remaining 18% of the adherent cells was dead. In the Petri dish, the alive cells were counted as 69 and the dead cells were counted as 17 of 86 total cells, which meant 80.2% of the adherent cells was alive and the remaining 19.8% of the adherent cells was dead. Figure 4.5, Figure 4.6, and Figure 4.7 show the first day images of the cells in organs on a chip. Figure 4.8, Figure 4.9, and Figure 4.10 show the first day images of the cells in the Petri dish.

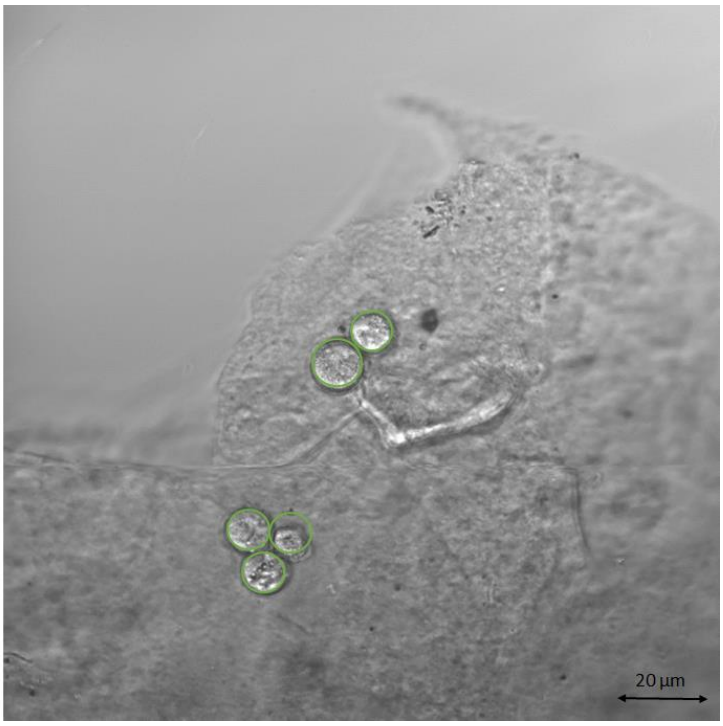

Figure 4.5: First image of first day of cells in the organs on a chip, counted 5 cells (100%) were alive.

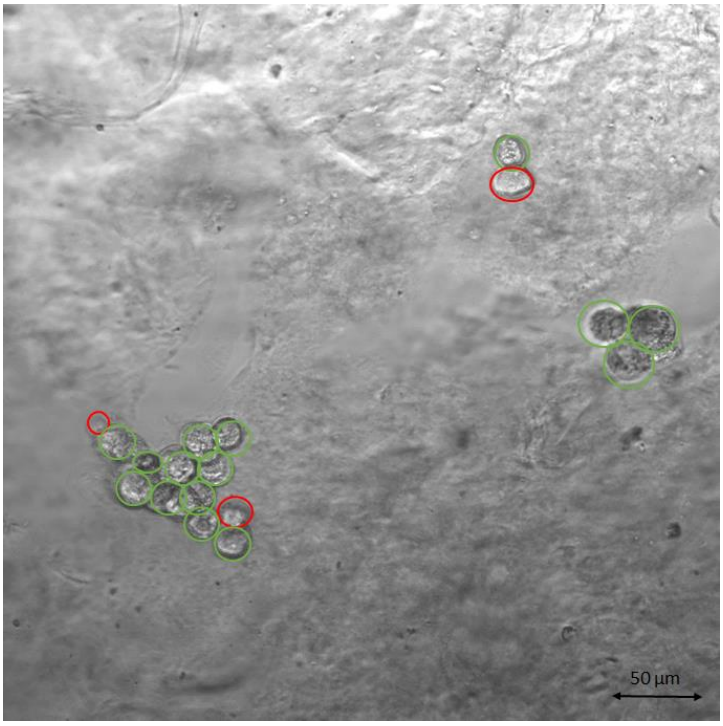

Figure 4.6: Second image of first day of cells in the organs on a chip system, 18 cells were counted, 15 cells (83.3%) were alive and 3 cells (16.7%) were dead.

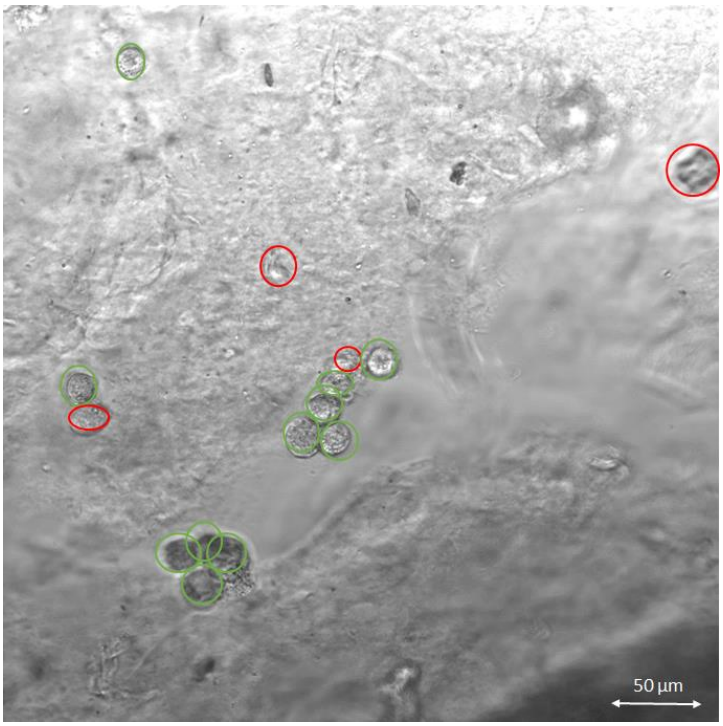

Figure 4.7: Third image of first day of cells in the organs on a chip system, 16 cells were counted, 13 cells (81.25%) were alive and 3 cells (18.75%) cells were dead.

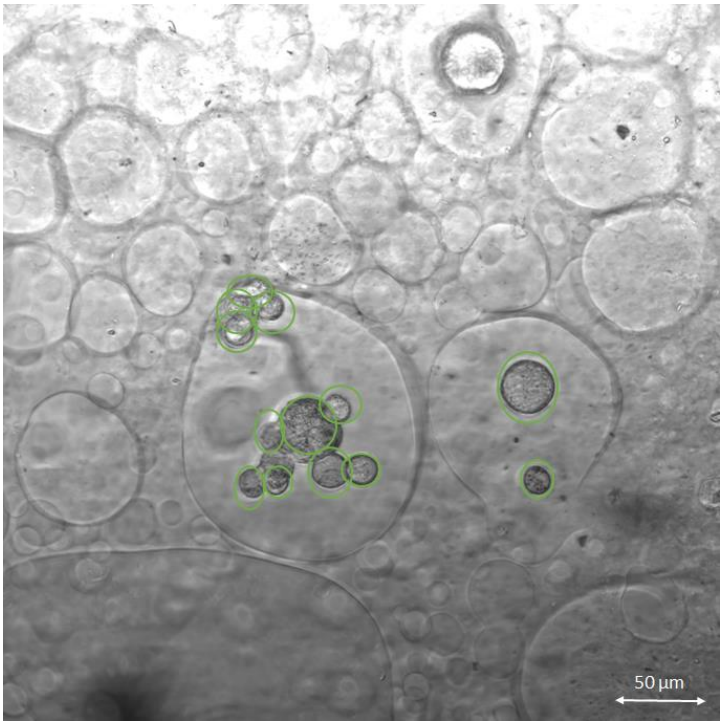

Figure 4.8: First image of first day of cells in the Petri, counted 15 cells (100%) were alive.

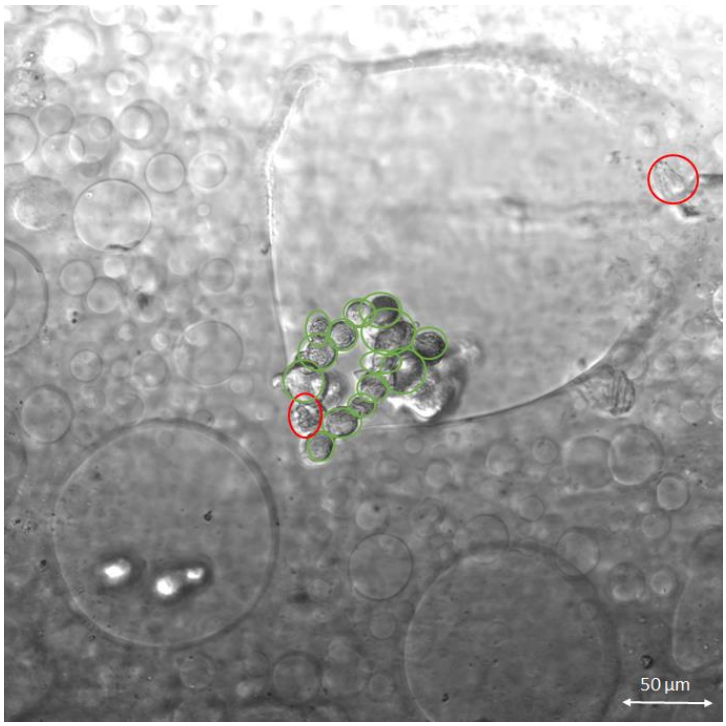

Figure 4.9: Second image of first day of cells in the Petri, 18 cells were counted, 16 cells (88.8%) were alive and 2 cells (11.2%) were dead.

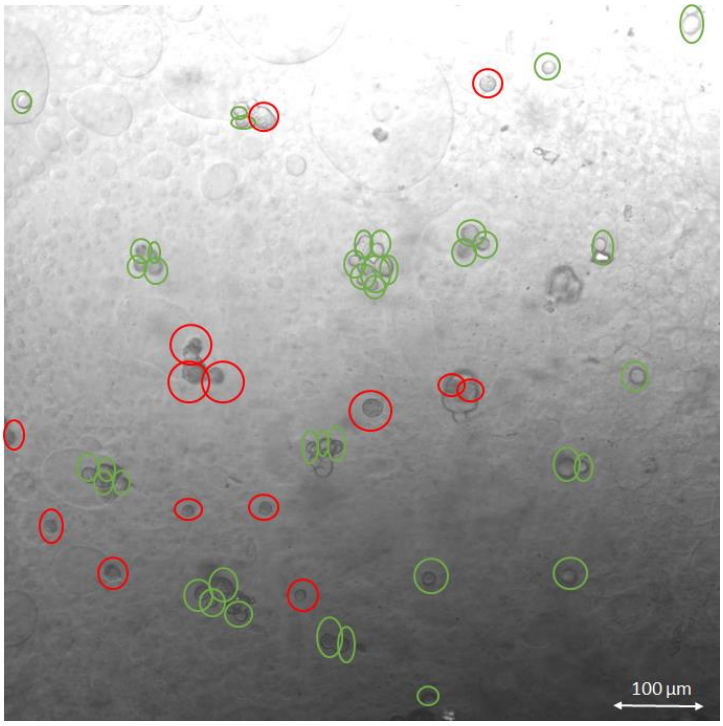

Figure 4.10: Third image of first day of cells in the Petri, 53 cells were counted, 38 cells (71.70%) was alive and 15 cells (28.30%) were dead.

After the completion of the image taking process, both chip and Petri was placed in incubator, and once more the organs on a chip platform was integrated with syringe pump for continuous feeding. Right after 48 hours, chip and Petri dish were again removed from incubator and placed on microscope orderly for third day imaging. In this process, amount of cell proliferation was calculated. Because, the cells were incubated for 2 days in an atmosphere of 5% CO_2 at 37 °C in incubator.

The amount of the cells in the scaffold that were on the organs on a chip was calculated as 98 on the third day. The total number of the alive cells were 88 (89.7%) and the dead cells were 10 (10.3%). On the other hand, the number of the cells in the scaffold, which were placed on the Petri was calculated as 18. In the Petri dish, 14 cells (77.8%) were alive and 4 cells (21.2%) were dead in the process of image taken. That was because the scaffold on the Petri has disassociated from surface and has floated on the medium. Thus, the lenses of the confocal microscopy could not catch an image since the scaffold was far from range of the lenses. Figure 4.11, Figure 4.12**,** and Figure 4.13 show the third day of cells in the organs on a chip platform and Figure 4.14 shows the third day of cells in the Petri.

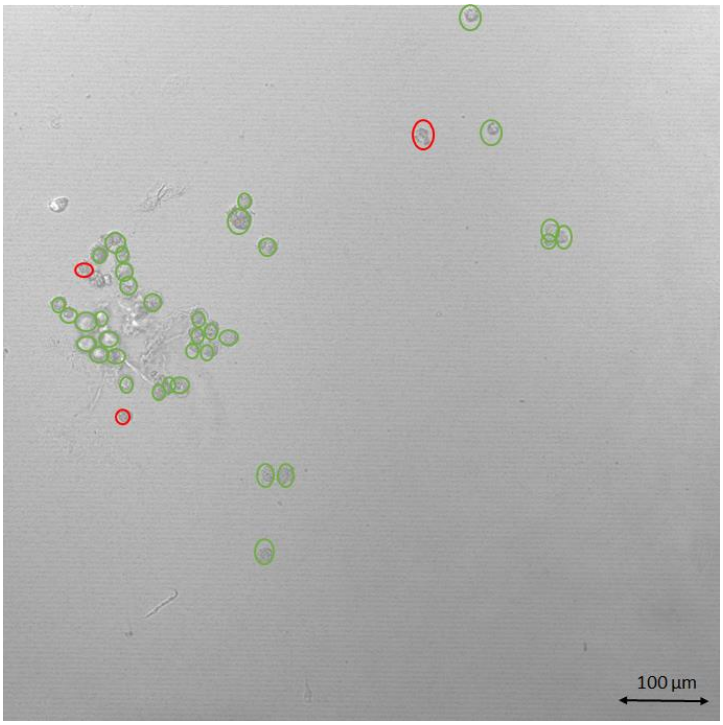

Figure 4.11: First image of third day of cells in the organs on a chip platform, 43 cells were counted, 38 cells (88.4%) were alive and 5 cells (11.6%) were dead.

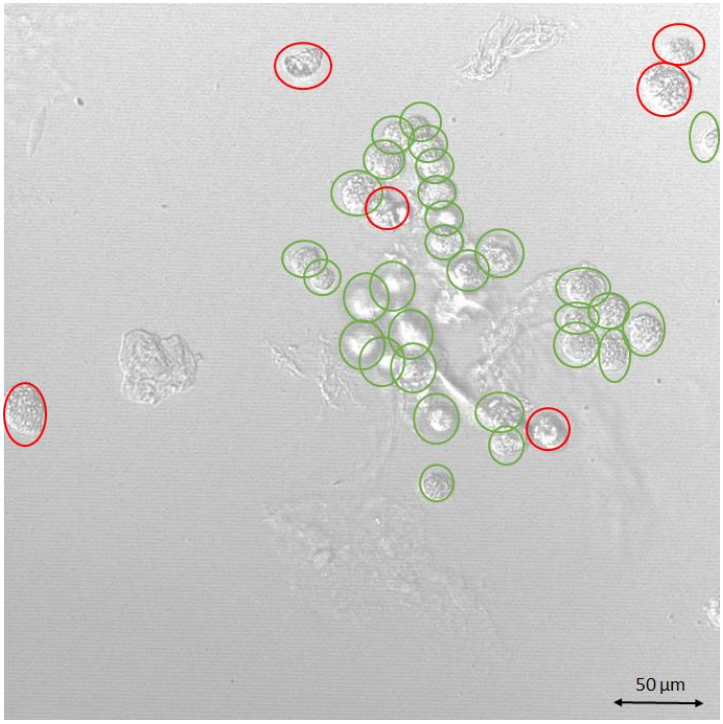

Figure 4.12: Second image of third day of cells in the organs on a chip platform, 36 cells were counted, 33 cells (91.7%) were alive and 3 cells (8.3%) were dead.

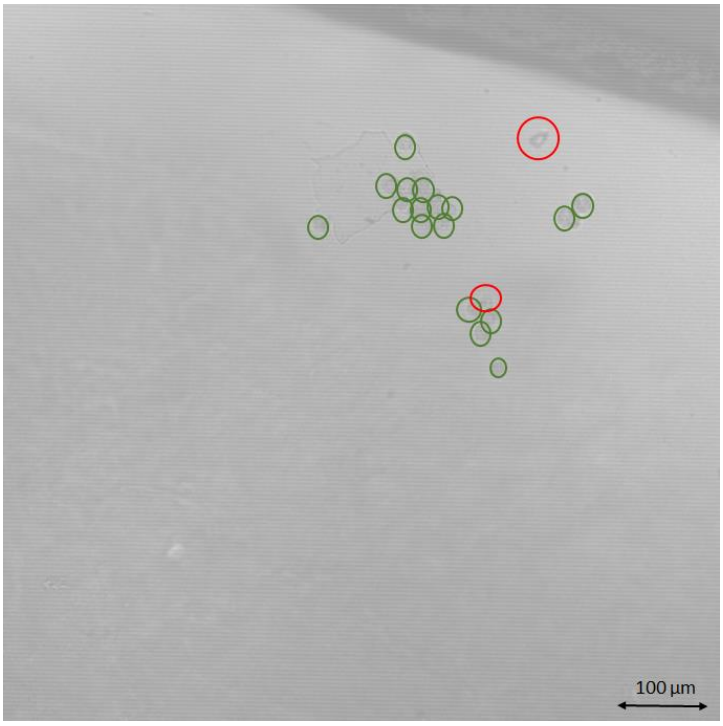

Figure 4.13: Third image of third day of cells in the organs on a chip platform, 19 cells were counted, 17 cells (89.5%) were alive and 2 cells (10.5%) cells were dead.

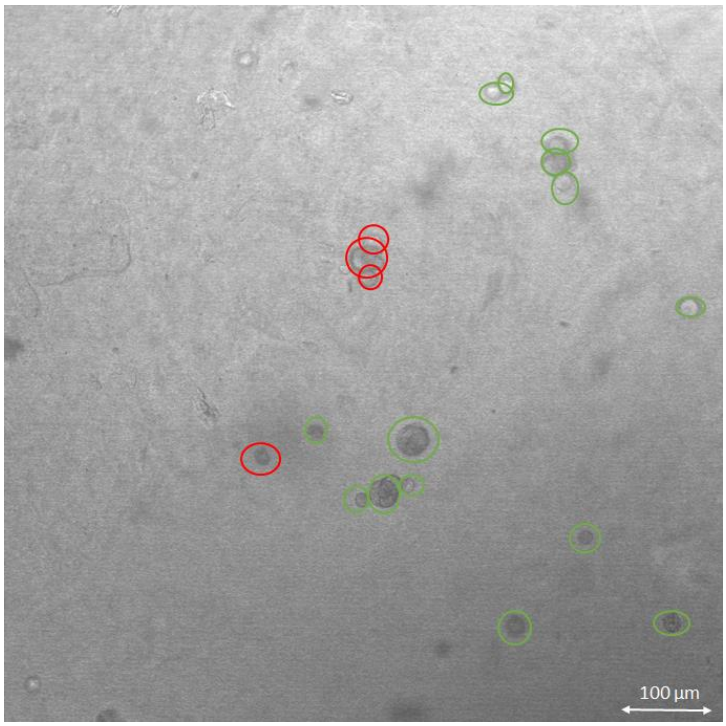

Figure 4.14: The image of third day image of cells in the Petri, 18 cells were counted, 14 cells (77.8%) were alive and 4 cells (21.2%) were dead.

Finally, the organs on a chip platform and the Petri dish was once more placed to the incubator and retrieved after 72 hours in order to obtain the images of the seventh day of the experiment. The counted number of the cells that were on the organs on a chip was 48. The total number of the alive cells were 42 (87.5%) and the dead cells were 6 (12.5%). Nonetheless, the cells in the scaffold that was on the Petri were counted as just 4. That was because the floating of the scaffold on the medium. The ratio of the alive cells was 50%.

Figure 4.15 and Figure 4.16 show the seventh day images of cells in the organs on a chip platform and Figure 4.17 shows the seventh day image of the cells in the Petri.

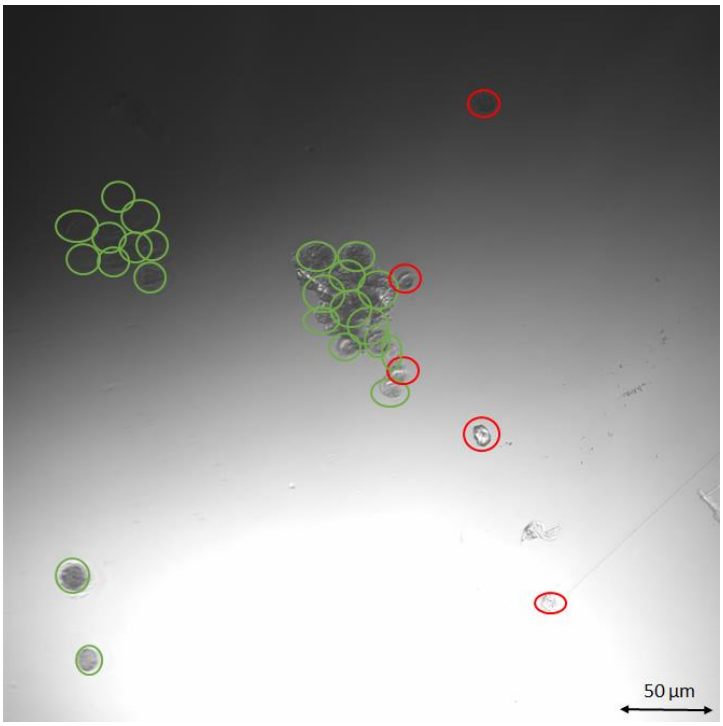

Figure 4.15: First image of seventh day of cells in the organs on a chip platform, 30 cells were counted, 25 cells (83.3%) were alive and 5 cells (16.7%) were dead.

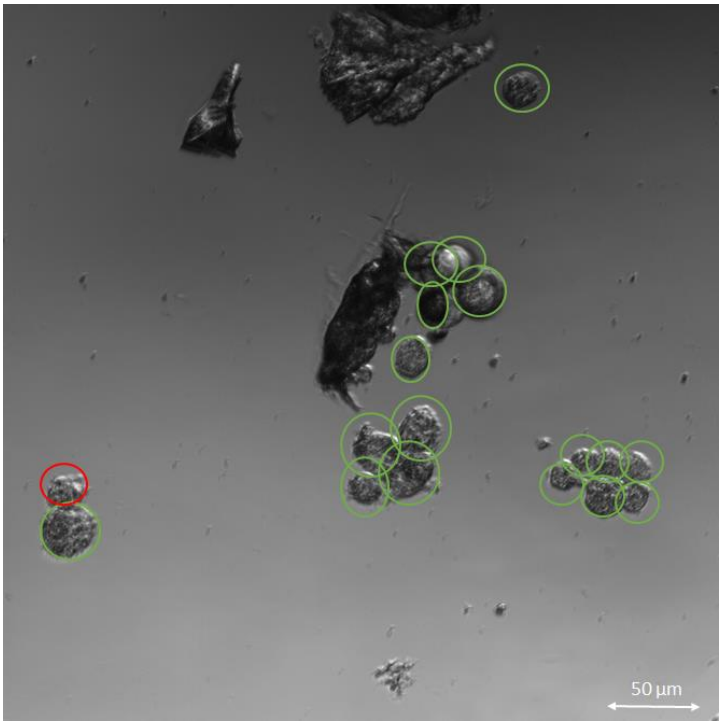

Figure 4.16: Second image of seventh day of cells in the organs on a chip platform, 18 cells were counted, 17 cells (94.4%) were alive and 1 cell (5.6%) was dead.

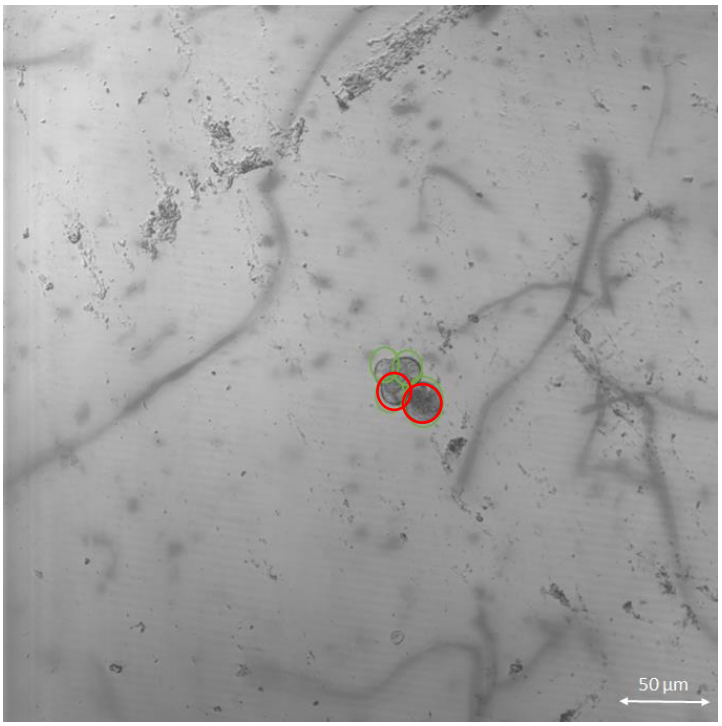

Figure 4.17: The image of third day of cells in the Petri, 4 cells were counted and 2 of the cells (50%) were dead and 2 of the cells (50%) were alive.

At the end of the experiment, the scaffolds and the remaining cells were removed from both organs on a chip platform and Petri. Then both of them was cleaned by using 70% of ethanol and UV application for 15 minutes in the biosafety cabinet.

Second part of the study was 10%-7% GelMA - alginate based tissue scaffold. Same as the first experiment, the organ on a chip platform acquired continuous feeding from the syringe pump. Both the chip and the Petri was placed to an incubator and retrieved to the confocal microscopy in order to obtain first, third- and seventh-day images. In the first day, adherence calculation was executed. 40 cells were found by the calculation for every μm^2. Thus, the number of the cells in both systems were counted. 37 cells were counted in the organs on a chip platform. The total number of the alive cells was 36 (97.3%) and the total number of the dead cells was 1 (2.7%). On the other hand, the total number of the adherent cells on the scaffold that was on the Petri dish was 25. The total number of the alive cells on the scaffold was 18 (72%) and the total number of the dead cells was 7 (28%).

Figure 4.18, Figure 4.19, and Figure 4.20 show the first day images of the cells in the organs on a chip platform and Figure 4.21, Figure 4.22, and Figure 4.23 show the first day images of the cells in the Petri dish.

Figure 4.18: First image of first day of cells in the organs on a chip platform, 10 cells were counted, all of the cells (100%) was alive.

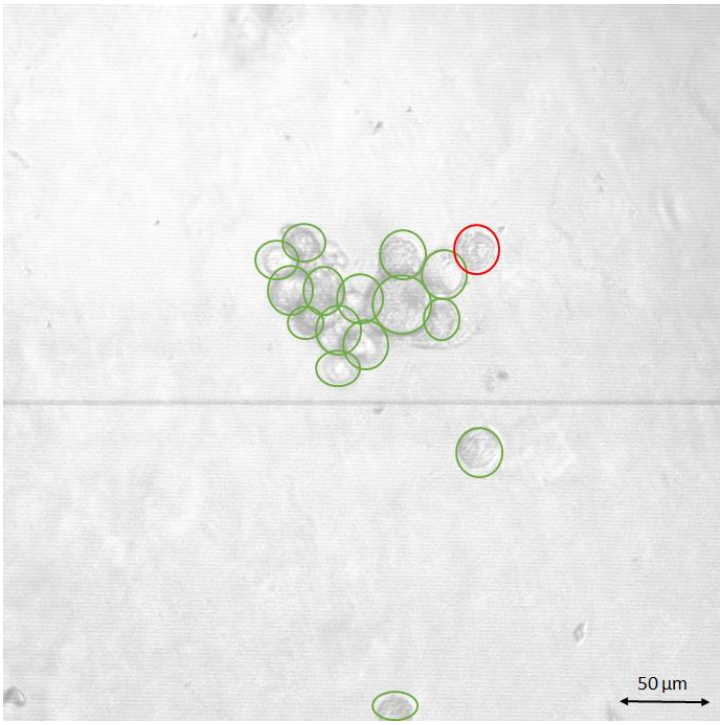

Figure 4.19: Second image of first day of cells in the organs on a chip platform, 16 cells were counted, 15 cells (93.7%) was alive and 1 cell (6.3%) was dead.

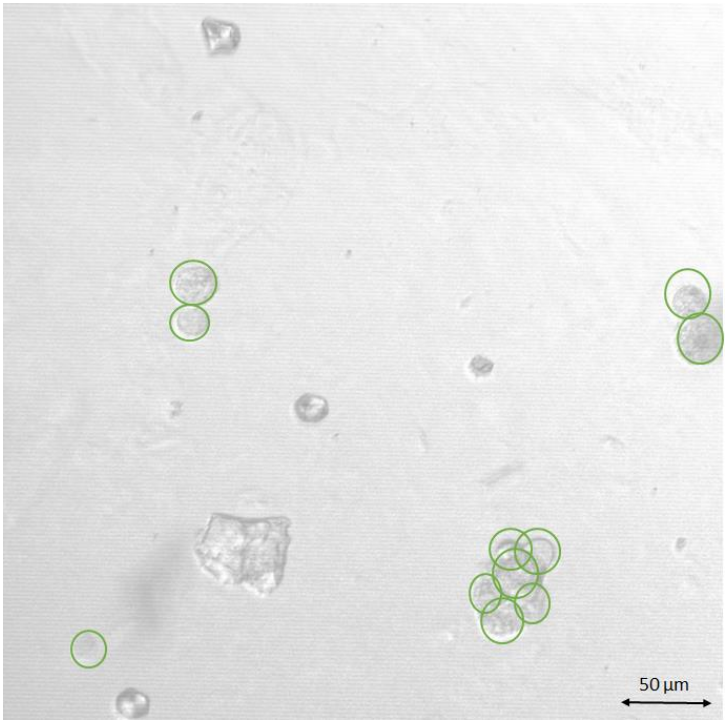

Figure 4.20: Third image of first day of cells in the organs on a chip platform, 11 cells were counted, all of the cells (100%) was alive.

Figure 4.21: First image of first day of cells in the Petri, 5 cells were counted, 4 cells (75%) were alive and 1 cell (25%) was dead.

Figure 4.22: Second image of first day of cells in the Petri, 9 cells were counted, 7 cells (77.8%) was alive and 2 cells (22.2%) were alive.

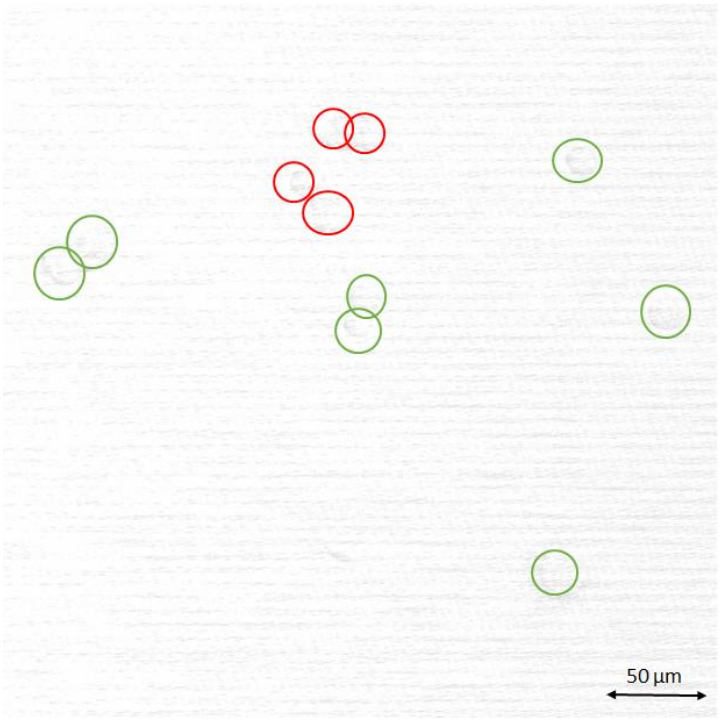

Figure 4.23: Third image of first day of cells in the Petri, 11 cells were counted, 7 cells (63.6%) were alive and 4 cells (36.4%) were dead.

After first day images are obtained from the organs on a chip platform and the Petri dish, they were placed back to incubator for 48 hours and then retrieved for confocal microscopy imagining again. The total number of the alive cells were counted as 56 (80%) and the total number of the dead cells were counted as 14 (20%) on the organs on a chip platform. On the other hand, the total number of the cells on the scaffold that was on the Petri dish was calculated as 18, 11 cells (61.1%) were alive and 7 cells (38.9%) were dead.

Figure 4.24, Figure 4.25, and Figure 4.26 for the organs on a chip platform and it was illustrated by Figure 4.27 for the Petri.

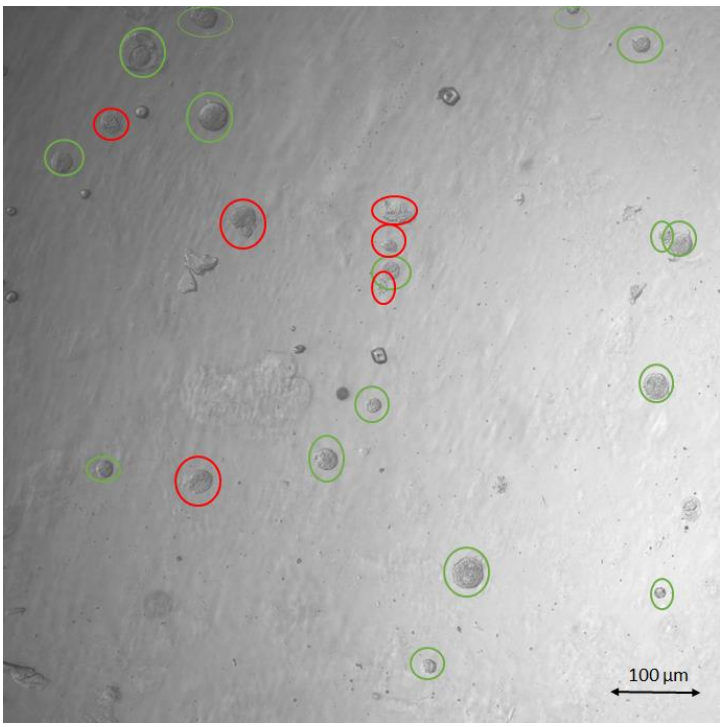

Figure 4.24: First image of third day of cells in the organs on a chip platform, 22 cells were counted, 16 cells (72.7%) were alive and 6 cells (27.3%) were dead.

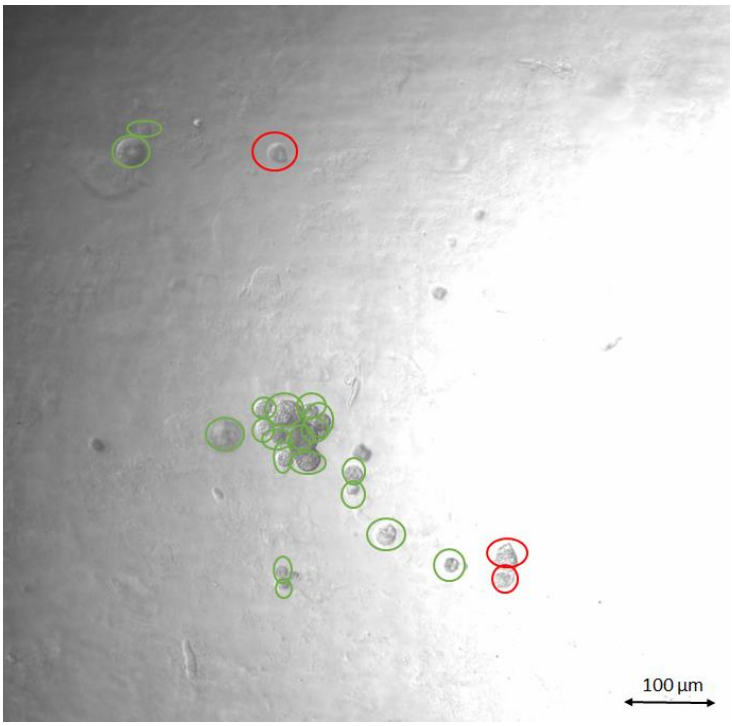

Figure 4.25: Second image of third day of cells in the organs on a chip platform, 22 cells were counted, 19 cells (86.4%) were alive and 3 cells (13.6%) were dead.

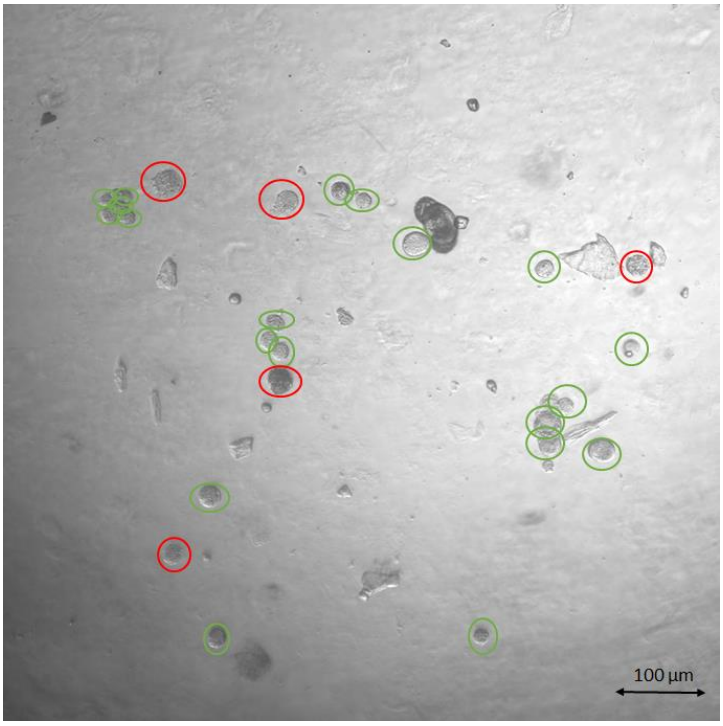

Figure 4.26: Third image of third day of cells in the organs on a chip platform, 26 cells were counted, 21 cells (80.8%) were alive and 5 cells (19.2%) were dead.

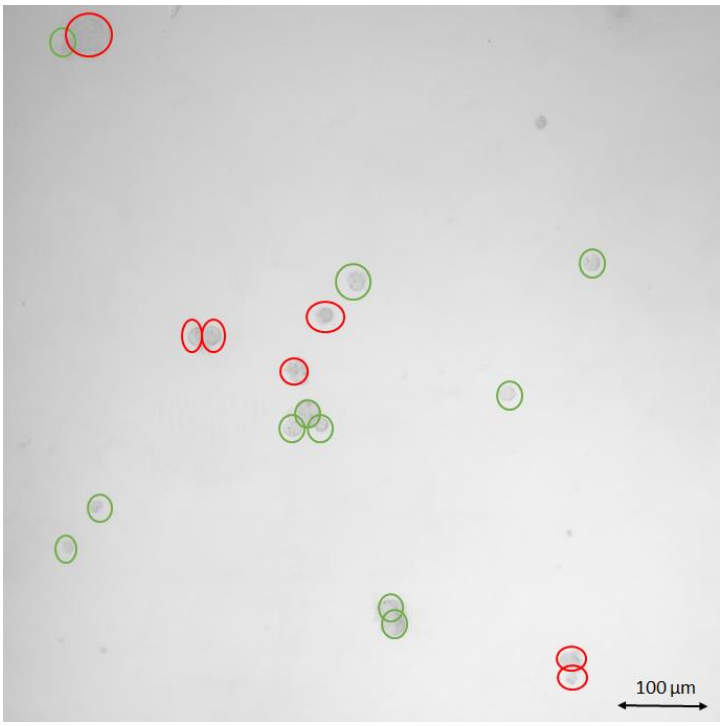

Figure 4.27: The image of third day of cells in the Petri, 18 cells were counted, 11 cells (61.1%) were alive and 7 cells (38.9%) were dead.

At seventh day, both systems were placed on microscopy and the images were taken. The total number of the cells on the scaffold that on the organs on a chip was 46 cells. 40 cells (87%) were alive and 6 cells (13%) were dead. On the other hand, the total number of the cells on the scaffold that were on the Petri dish was 12 cells. The alive cells were 5 (41.7%) and 7 cells (58.3%) were dead.

Figure 4.28 represents the seventh day image of the organs on a chip platform and Figure 4.29 represents the seventh day image of the Petri.

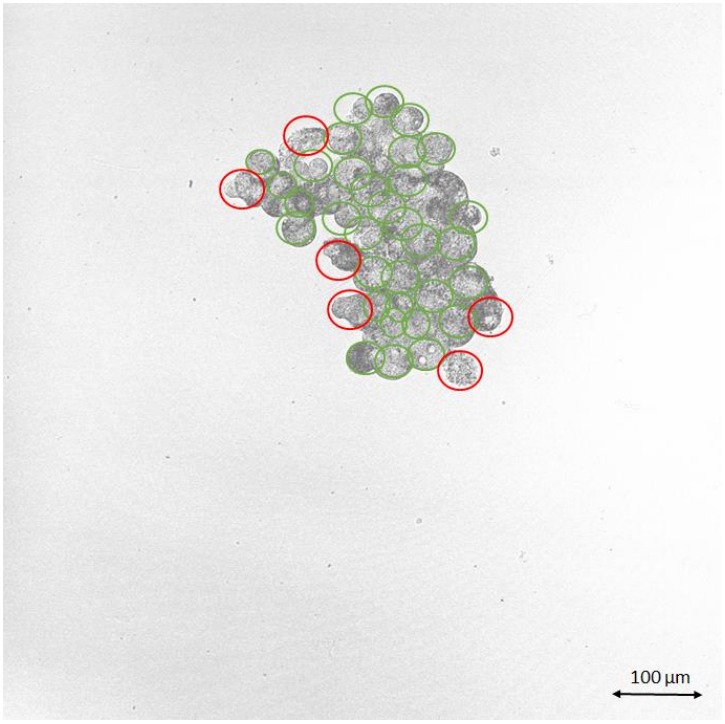

Figure 4.28, The image of seventh day of cells in the organs on a chip platform, 46 cells were counted, 40 cells (87%) were alive and 6 cells (13%) were dead.

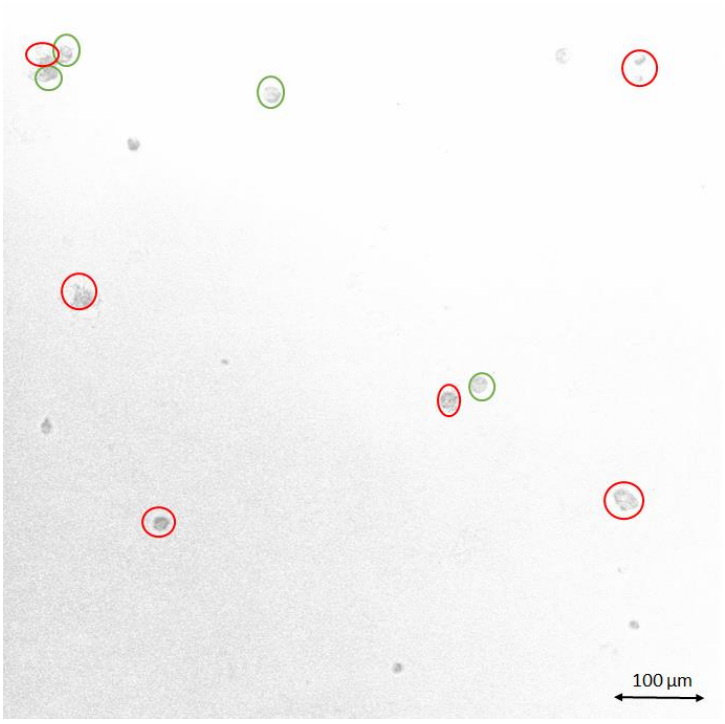

Figure 4.29: The image of seventh day of cells in the Petri, 12 cells were counted, 5 cells (41.7%) were alive and 7 cells (58.3%) were dead.

5. RESULTS and DISCUSSION

In the first experiment of this study, 7%-5% GelMA-alginate containing scaffolds were used in the organs on a chip and in the Petri dish. The scaffolds were so important, since they have played the role as mimicking the skin tissue for cell proliferation. The scaffolds were stood still in the surface of the Petri and organs on a chip system, lots of cells had been attached to the scaffold, which can be seen from first day images. The quality of 7%-5% GelMA-alginate containing scaffold was better in terms of shape, angles, and curves compared to 10%-7% GelMA-alginate containing scaffold.

The scaffold on the organs on a chip platform has shown more stability compared to the Petri dish. Because, on the third day, some of the scaffold parts on the Petri has disassociated from the surface and commenced floating on the medium. That was caused by medium in the Petri. The scaffold was composed of GelMA and alginate. Alginate has shown swelling in the presence of constant medium. On the other hand, there was continuous and fixed flow in the organs on a chip from inlet channel to outlet channel, which prevented accumulation of high amount of medium in the system. Even if the scaffold in the chip system has shown swelling, it was not dissociated from the surface of the chip.

In the chip system, the reaction chamber that contained cells was fed continuously via syringe pump as 1 ml/h. That flow provided not only fresh medium for cells but also expurged the stale (relatively) and the dead cells out of the reaction chamber. Moreover, the average percentage of the alive cells was higher in the organs on a chip platform as well as the percentage of the alive cells on first, third, and seventh day individually. It was calculated as 163 (88%) alive and 22 (12%) dead cells of 185 total cells in the organs on a chip. In the Petri dish, it was observed that 85 (78.7%) cells were alive and 23 (21.3%) cells were dead of 108 total cells.

Figure 5.1 shows the alive cell ratio in the both platforms with 7% - 5% GelMA – alginate containing scaffold.

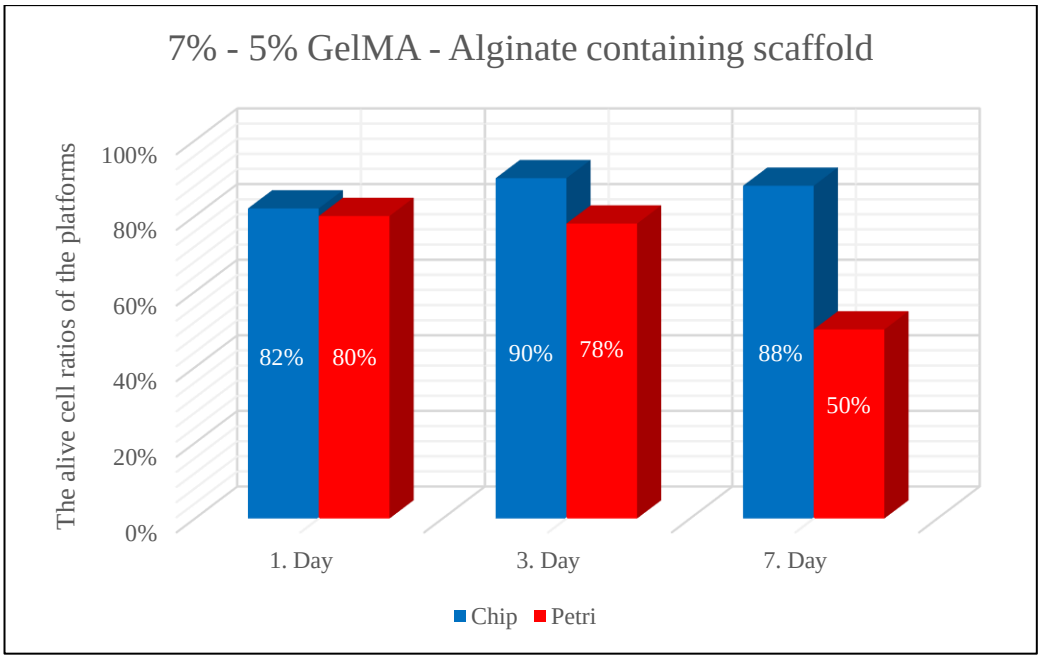

Figure 5.1: The percentage comparison of the adherence of the cells in both systems.

In the second experiment that was composed of 10% - 7% GelMA – Alginate containing scaffold the organs on a chip was more successful compared to the Petri dishes. The organs on a chip was better in terms of the total number of alive cells and the general composition of the scaffold. The ratio of the alive cells in the organs on a chip was 86.3%, 132 alive cells of 153 cells, which was only 61.8%, 34 alive cells of 55 cells in the Petri dish. Figure 5.2 shows the alive cell ratio in the both platforms with 10% - 7% GelMA – alginate containing scaffold.

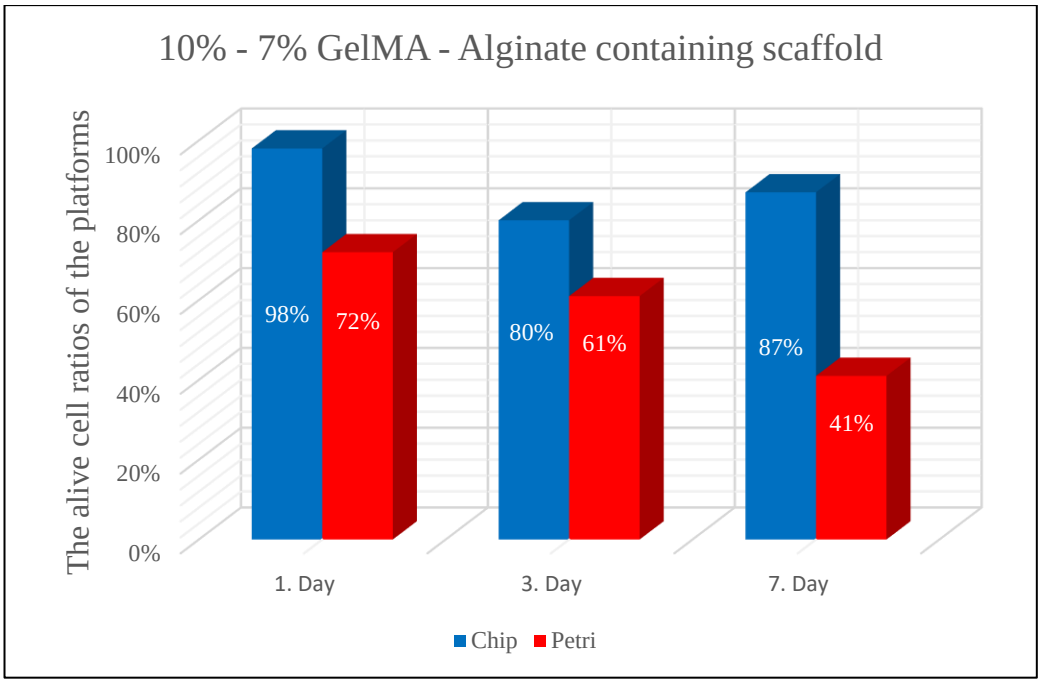

Figure 5.2: The alive cell ratios of the platforms

In the scaffolds, 10% - 7% GelMA – alginate containing scaffold has shown more stability compared to 7% - 5% one. Because, amount of GelMA has provided more effective cross-linking process and alginate has provided more rapid polymerization of gelation. It has led more stable construction. Besides, the scaffolds did not affect the cell viability in the organs on a chip system. The ratios were similar to each other. On the other hand, the alive cell ratio was better in the Petri dish with 7%- 5% GelMA – alginate containing scaffold in 1st, 3rd, and, 7th days compared to 10%- 7% GelMA – alginate containing scaffold.

That was because of amount of alginate in the system. 10% amount showed toxicity towards cells. There were some disassociation parts in the scaffold in the presence of the medium. In contrast, 10% alginate did not show toxicity in the organs on a chip platform, because the flow of the medium was continuous and no accumulation of the medium was not observed, which prevented the disruption of the integrity. Figure 5.3 shows the comparison between the scaffolds of 10% - 7% GelMA – alginate and 7% - 5% GelMA – alginate and Figure 5.4 shows the alive cell ratios in the Petri dishes with two different scaffolds.

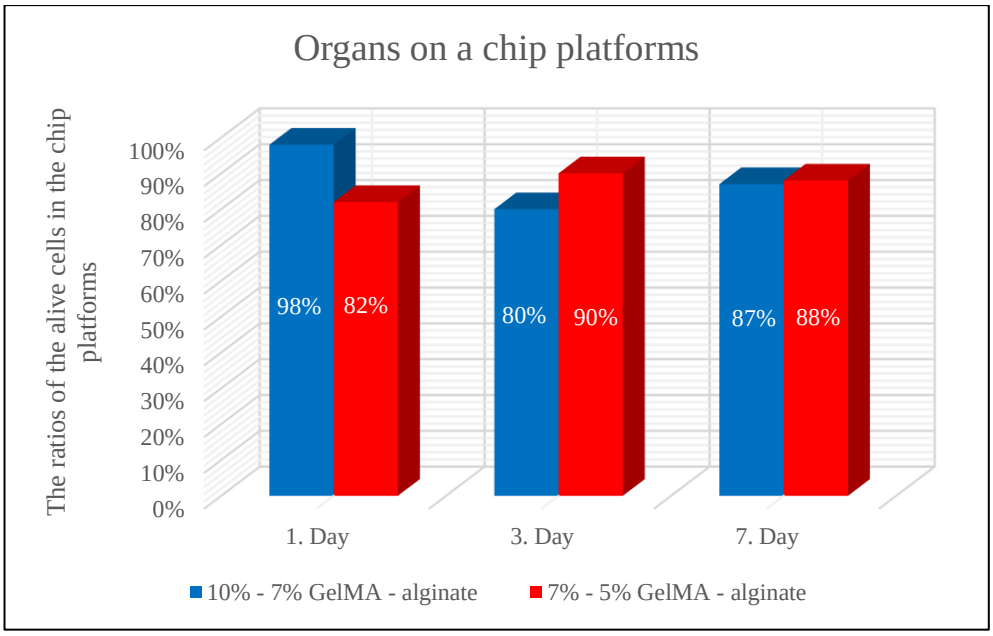

Figure 5.3: The alive cell ratios in the scaffolds.

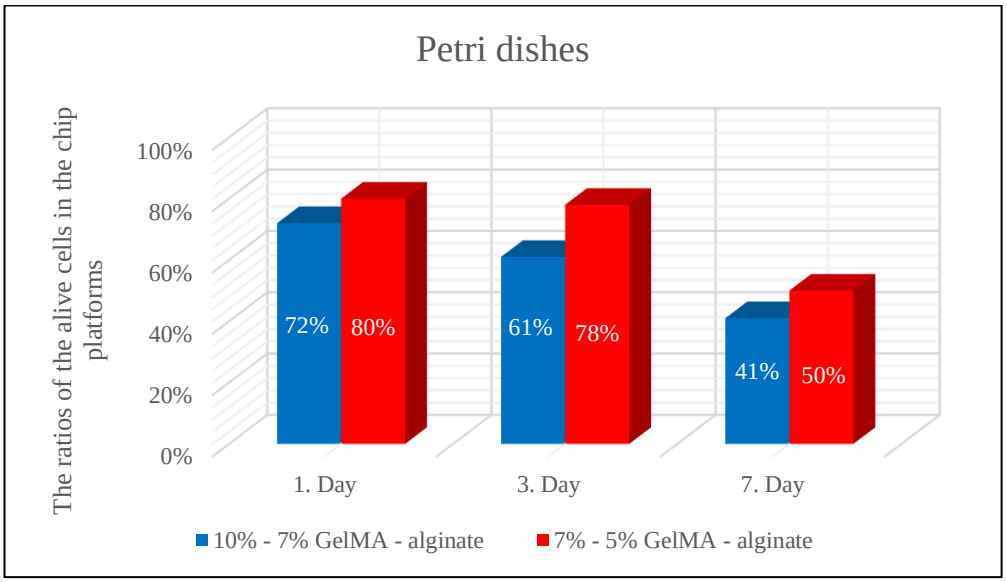

Figure 5.4: The alive cell ratios in the Petri dishes.

Lastly, as it was illustrated before, 7% - 4% and 5% - 4% GelMA – alginate containing mixture has failed during bio printing process. Both mixtures have shown instability and fluidity behavior. Because, the both GelMA and alginate content was insufficient. GelMA was not sufficient to be initiated rapid cross-linking reaction to link alginate. Alginate was not sufficient to undergo gelation process and link with GelMA [47]. Therefore, the mixtures could not be printed in desired shape and viscosity.

6. CONCLUSION

Microfluidic systems are composed of most advanced implementations of several engineering disciplines such as material sciences and engineering, chemical engineering, and bioengineering. After the fabrication of these systems become popular, it has gained wide range of utilizing area, which can be sorted as lab-on-a-chip, biosensors, and most novel one organ-on-a-chip technologies. In this study, PMMA was utilized as main material of the skin-on-a-chip. It was fabricated ten-layered structure, which could permit mimicking different layers of the skin, which are hypodermis, dermis, and epidermis layers. Eight holes in the same size were inserted in the system during the design in order to provide easy integration and disintegration for reproducibility. The bolts were used to integrate the layers of the chip. Besides, two different scaffolds that consisted of GelMA and Sodium Alginate mixture with different proportions were printed by utilizing bio printer in order to mimic ECM for creating natural cell environment.

There were two stages of the study. The first one was comparing the organs on a chip platform that allows 3D cell culturing with a Petri dish that allows only 2D cell culture studies. Both of them utilized 7% - 5% GelMA - alginate mixture. The second experiment compared the organs on a chip system with a Petri dish. Again, the main purpose was to compare the effectiveness of 3D cell culture against 2D cell culture techniques. In this part of the study as a tissue scaffold 10% - 7% GelMA - alginate solution was used. In all experiments, mouse fibroblast cells were used for cell culturing.

The main objectives of this study were proof-of-concept of the organs on a chip and making comparison between two different scaffolds contents. The organs on a chip platform was unique in terms of utilized material, shape, size, and integration ability of its kind. The platform was developed as 10 layer that were composed of 4 smooth layer, 3 reaction chambers with inlet channels, and 3 reaction chambers with outlet channels. In total, the chip has had 3 different reaction chambers in it, which can mimic skin construction as hypodermis, dermis, and epidermis. The layers have been designed with bolts insertion. That was executed in order to provide easy to integrate and disintegrate, which offers easy and precise sterilization, interference during the experiment, and additive modification on the platform. Furthermore, PMMA was

utilized for material of the organs on a chip platform. It was selected because of its high chemical and mechanical durability, low-cost obtainment and, fabrication processes. PMMA requires no surface characterization a feature absent in PDMS, which is mostly utilized material in the microfluidic researchers. Therefore, cell viability results have shown that the organs on a chip was clearly successful in implementations.

The chip system has shown more stability in the preservation of the scaffold as a whole and some cells were observed on the surface of the PMMA chip. Furthermore, continuous feeding has provided more cell viability and colonization on organs on a chip platform. The work was unique in terms of being three-layered for different cell cultures, using PMMA instead of PDMS.

Finally, in case the further and more detailed optimizations such as optimizing the cell chamber dimeter, width of the inlet and outlet channels, tighter integration of the layers and the flow rate of the medium from injection pump are done, much more successful organs on a chip platform may be realized. If the abovementioned enhancements can be executed, the chip will present a great promise to use as a platform for drug delivery, drug toxicity, and drug effectivity testing instead of animal models, cosmetics toxicity testing, disease modelling and most importantly personal-oriented disease modelling.

REFERENCES

[1] Abaci H.E., et al., (2015), "Pumpless microfluidic platform for drug testing on human skin equivalents.", Lab on a Chip. 15 (3): p. 882-888.

[2] Abbott A., (2003), "Biology's new dimension." Nature Publishing Group.

[3] Abgrall P. and N.T. Nguyen, (2008), "Nanofluidic devices and their applications.", Analytical chemistry. 80 (7): p. 2326-2341.

[4] Alexander F., S. Eggert, and J. Wiest, (2018), "Skin-on-a-chip: transepithelial electrical resistance and extracellular acidification measurements through an automated air-liquid interface.", Genes. 9 (2): p. 114.

[5] Ashammakhi N., et al., (2019), "Bioinks and bioprinting technologies to make heterogeneous and biomimetic tissue constructs.", Materials Today Bio. 1: p. 100008.

[6] Ataç B., et al., (2013), "Skin and hair on-a-chip: in vitro skin models versus ex vivo tissue maintenance with dynamic perfusion.", Lab on a chip. 13 (18): p. 3555-3561.

[7] Avci H., et al., (2017), "Recent Advances in Organ-on-a-chip Technologies and Future Challenges: A Review.", Turkish Journal of Chemistry. 42: p. 587-610.

[8] Bertassoni L.E., et al., (2014), "Direct-write bioprinting of cell-laden methacrylated gelatin hydrogels.", Biofabrication. 6 (2): p. 024105.

[9] Bhise N.S., et al., (2014), "Organ-on-a-chip platforms for studying drug delivery systems.", Journal of Controlled Release. 190: p. 82-93.

[10] Biolabs C. 2D vs 3D. (2017); Available from: https://www.creative-biolabs.com/adc/2d-vs-3d.htm.

[11] Carlsson J. and J. Yuhas, (1984), "Liquid-overlay culture of cellular spheroids, in Spheroids in cancer research.", Springer. p. 1-23.

[12] DiMasi J.A., et al., (2010), "Trends in risks associated with new drug development: success rates for investigational drugs.", Clinical Pharmacology & Therapeutics. 87 (3): p. 272-277.

[13] DiMasi J.A. and H.G. Grabowski, (2007), "The cost of biopharmaceutical R&D: is biotech different? Managerial and decision Economics.", 28 (4-5): p. 469-479.

[14] DiMasi J.A., R.W. Hansen, and H.G. Grabowski, (2003), "The price of innovation: new estimates of drug development costs.", Journal of health economics. 22 (2): p. 151-185.

[15] Ghaemmaghami A.M., et al., (2012), "Biomimetic tissues on a chip for drug discovery.", Drug discovery today. 17 (3-4): p. 173-181.

[16] Goddard III W.A., et al., (2007), "There's Plenty of Room at the Bottom: An Invitation to Enter a New Field of Physics." in Handbook of Nanoscience, Engineering, and Technology, CRC Press. p. 27-36.

[17] Griffith L.G. and G. Naughton, (2002), "Tissue engineering--current challenges and expanding opportunities.", science. 295 (5557): p. 1009-1014.

[18] Harrison R.G., (1910), "The outgrowth of the nerve fiber as a mode of protoplasmic movement." Journal of Experimental Zoology. 9 (4): p. 787-846.

[19] Harrison R.G., et al., (1907), "Observations of the living developing nerve fiber. The Anatomical Record.", 1 (5): p. 116-128.

[20] Hopkins A.L., (2008), "Network pharmacology: the next paradigm in drug discovery.", Nature chemical biology. 4 (11): p. 682.

[21] Huh D., G.A. Hamilton, and D.E. Ingber, (2011), "From 3D cell culture to organs-on-chips.", Trends in cell biology. 21 (12): p. 745-754.

[22] Huh D., et al., (2010), "Reconstituting organ-level lung functions on a chip.", Science. 328 (5986): p. 1662-1668.

[23] Hull C.W., (1986), "Apparatus for production of three-dimensional objects by stereolithography.", Google Patents.

[24] Hutchinson L. and R. Kirk, (2011), "High drug attrition rates—where are we going wrong?", Nature Publishing Group.

[25] Judy J.W., (2001), "Microelectromechanical systems (MEMS): fabrication, design and applications." Smart materials and Structures. 10 (6): p. 1115.

[26] Kola I., (2008), "The state of innovation in drug development. Clinical Pharmacology & Therapeutics.", 83 (2): p. 227-230.

[27] Kola I. and J. Landis, (2004), "Can the pharmaceutical industry reduce attrition rates?", Nature reviews Drug discovery. 3 (8): p. 711.

[28] Langer R. and D.A. Tirrell, (2004), "Designing materials for biology and medicine.", Nature. 428 (6982): p. 487.

[29] Lee J., M.J. Cuddihy, and N.A. Kotov, (2008), "Three-dimensional cell culture matrices: state of the art.", Tissue Engineering Part B: Reviews. 14 (1): p. 61-86.

[30] Lee S., et al., (2017), "Construction of 3D multicellular microfluidic chip for an in vitro skin model.", Biomedical microdevices. 19 (2): p. 22.

[31] Liu W., et al., (2018), "Coaxial extrusion bioprinting of 3D microfibrous constructs with cell-favorable gelatin methacryloyl microenvironments. Biofabrication.", 10 (2): p. 024102.

[32] Mastrangelo C.H., M.A. Burns, and D.T. Burke, (1998), "Microfabricated devices for genetic diagnostics.", Proceedings of the IEEE. 86 (8): p. 1769-1787.

[33] Matellan C. and E. Armando, (2018), "Cost-effective rapid prototyping and assembly of poly (methyl methacrylate) microfluidic devices.", Scientific reports. 8 (1): p. 6971.

[34] Michalski M.H. and J.S. Ross, (2014), "The shape of things to come: 3D printing in medicine.", Jama. 312 (21): p. 2213-2214.

[35] Moore G.E., (1965), "Cramming more components onto integrated circuits.", McGraw-Hill New York, NY, USA:.

[36] Nakamura M., et al., (2010), "Biomatrices and biomaterials for future developments of bioprinting and biofabrication.", Biofabrication. 2 (1): p. 014110.

[37] Pangalos M.N., L.E. Schechter, and O. Hurko, (2007), "Drug development for CNS disorders: strategies for balancing risk and reducing attrition.", Nature Reviews Drug Discovery. 6 (7): p. 521.

[38] Ren K., J. Zhou, and H. Wu, (2013), "Materials for microfluidic chip fabrication.", Accounts of chemical research. 46 (11): p. 2396-2406.

[39] Roth A. and T. Singer, (2014), "The application of 3D cell models to support drug safety assessment: opportunities & challenges.", Advanced drug delivery reviews. 69: p. 179-189.

[40] Santini J., John T, et al., (2000), "Microchips as controlled drug-delivery devices.", Angewandte Chemie International Edition. 39 (14): p. 2396-2407.

[41] Selimović Š., M.R. Dokmeci, and A. Khademhosseini, (2013), "Organs-on-a-chip for drug discovery." Current opinion in pharmacology. 13 (5): p. 829-833.

[42] Seyedmahmoud R., et al., (2019), "Three-Dimensional Bioprinting of Functional Skeletal Muscle Tissue Using Gelatin Methacryloyl-Alginate Bioinks.", Micromachines. 10 (10): p. 679.

[43] Tabeling P., (2005), "Introduction to microfluidics.": OUP Oxford.

[44] Tan H.Y., W.K. Loke, and N.-T. Nguyen. (2010), "Integration of PDMS and PMMA for batch fabrication of microfluidic devices.", in 6th World Congress of Biomechanics (WCB 2010). August 1-6, 2010 Singapore. Springer.

[45] Wang W. and S.A. Soper, (2006), "Bio-MEMS: technologies and applications.",: CRC press.

[46] Wufuer M., et al., (2016), "Skin-on-a-chip model simulating inflammation, edema and drug-based treatment.", Scientific reports. 6: p. 37471.

[47] X Chen Y., B. Cain, and P. Soman, (2017), "Gelatin methacrylate-alginate hydrogel with tunable viscoelastic properties.", AIMS Materials Science. 4 (2).

[48] Zahn J.D., (2009), "Methods in bioengineering: biomicrofabrication and biomicrofluidics.",: Artech House.

[49] Zhang X., et al., (2018), "Marine Biomaterial-Based Bioinks for Generating 3D Printed Tissue Constructs." Marine drugs. 16 (12): p. 484.

BIOGRAPHY

Ahmet Akif KIZILKURTLU was born in İstanbul in 8 October, 1994. He has studied primary and secondary education in Doktor Tevfik Sağlam İlköğretim Okulu. After the completion of high school education in Özel Çınar Koleji, he has registered bioengineering program of faculty of engineering and natural sciences in Uskudar University. He has graduated from there with honors degree. After that, he has registered the master program of biotechnology in Gebze Technical University.